Motorcycle Modeling and Control

W. Ooms BSc.

DCT 2011.014

Master's thesis

Coach(es): Dr. Ir I.J.M. Besselink

Supervisor: Prof. Dr. H. Nijmeijer

Technische Universiteit Eindhoven
Department Mechanical Engineering
Dynamics and Control Group

Eindhoven, February 21, 2011

Preface

Hereby, I would like to thank a couple persons who helped and supported me during the research I performed for my final Master project at the department Mechanical Engineering of the Eindhoven University of Technology. This is my second graduation project since the first one was prematurely discontinued. Therefore, I still haven't had a chance to thank the people from the first graduation project. Herewith, I like to thank the following people for their support: My first coach Theo Hofman, the team members Bas Laugeman, Gijs Peeters, Sebastiaan van der Tas, Erik van Meijl, other members of the TU/e Hybrid TukTuk Team and the staff of the AES laboratory. From my second graduation project, I'd like to thank Igo Besselink and Henk Nijmeijer for giving me the oppertunity to do research in the field of motorcycle dynamics. I believe that the manned missile, the airborne motorcycle, is the future. Furthermore, I'd like to thank my brother Sidney Ooms, my sisters Jordi and Gabi Ooms, and my parents Clari and Henk Ooms for their great mental support during the difficult transition period between the projects.

July, 2010,

Wesley Ooms

Summary

An 11 degree of freedom motorcycle model that is capable of predicting the dynamic behavior of a motorcycle is derived in this report. The 11 degrees of freedom are the position and orientation of the main body in three dimensional space, the front and rear suspension deflection, the rotation of the front and rear wheel and the steering angle. With these 11 degrees of freedom, the model is accurate enough to predict the motorcycle dynamics, including the tyre dynamics, yet small enough to be used and implemented in an onboard electronic control unit.

The method of deriving the equations of motion is borrowed from robot modeling and starts with defining the important parameters and generalized coordinates. The model has 11 generalized coordinates and approximately 70 model parameters. With these coordinates and parameters, an expression for the mass center position vectors, rotation point position vectors and force target position vectors is derived. With these vectors available, the complete set of equations of motion is derived.

The equations of motion are implemented in a Simulink model and simulated. The equations of motion are linearized and compared with other linear models from literature. This comparison shows a good agreement. Also, the nonlinear model is validated against two other models from literature. From this comparison, it can be concluded that the model is correct and accurate.

After a complete and thorough validation, the model is used to design a reference trajectory tracking controller. The controller employs state feedback with proportional gain. With the state feedback controller, the motorcycle is stable in a forward velocity range from 1 meter per second up to 100 meter per second and camber angles between -70 and +70 degrees, if the tyre lateral friction allows this. Stability of the motorcycle at large variations in acceleration is not investigated. The stabilized motorcycle can be controlled to follow a certain path in the ground plane. The controller can track this path within an accuracy of a few centimeters.

Samenvatting

Een 11 graden van vrijheid motorfietsmodel dat in staat is om het dynamisch rijgedrag van de motorfiets te voorspellen is in dit verslag afgeleid. Deze 11 vrijheidsgraden zijn de positie en oriëntatie van de motorfiets in de driedimensionale ruimte, de voor- en achtervering, de rotatie van het voor en achterwiel en de stuurhoek. Het motorfietsmodel is met deze 11 vrijheidsgraden nauwkeurig genoeg om de dynamica van de motorfiets te voorspellen, inclusief de dynamica van de banden, en tegelijkertijd is het klein genoeg om gebruikt en geïmplementeerd te worden in een regelsysteem op de motorfiets.

De manier van modelleren vindt zijn oorsprong in de robotica en begint met het definiëren van de benodigde parameters en gegeneraliseerde coördinaten. Het motorfiets model heeft 11 gegeneraliseerde coördinaten en ongeveer 70 parameters. Met deze coördinaten en parameters worden de positievectors van de massamiddelpunten en rotatiepunten en de punten waar krachten aangrijpen beschreven in de vorm van een wiskundige vergelijking. Deze positievectors worden vervolgens gebruikt om de bewegingsvergelijkingen van Lagrange af te lijden.

De bewegingsvergelijkingen zijn in Matlab/Simulink geïmplementeerd en gesimuleerd. De bewegingsvergelijkingen zijn eveneens gelineariseerd en vergeleken met andere lineaire motorfietsmodellen uit de literatuur. De modellen uit de literatuur en dit model geven vergelijkbare resultaten. Het niet-lineaire model is ook vergeleken met twee andere niet lineaire modellen uit de literatuur. Ook deze vergelijking laat zien dat het model correct en nauwkeurig is.

Nadat het model grondig gevalideerd is, is het model gebruikt om een stabiliserende regelaar te ontwerpen die het motorfietsmodel een referentietraject in het grondvlak laat volgen. De regelaar koppelt de te regelen toestand van het systeem terug naar het stuurkoppel. De motorfiets is met deze regelaar stabiel bij een voorwaartse snelheid van 1 meter per seconde tot minimaal 100 meter per seconde en rolhoeken van de motorfiets tot 70 graden, mits de grip van de banden groot genoeg is. De gestabiliseerde motorfiets kan aangestuurd worden om een bepaald traject te volgen met een afwijking van slechts enkele centimeters.

List of Symbols

C	Christoffel matrix	
F	force	
I	rotational inertia	
M	mass matrix	
O	position vector	
P	potential energy vector	
Q	virtual work	
R	rotation matrix	
T	torque vector	
W	external work vector	
b_1	rear tire vertical damping constant	
b_2	rear suspension vertical damping constant	
b_3	front suspension vertical damping constant	
b_4	front tire vertical damping constant	
b_{lr}	rear tire longitudinal damping constant	
b_{tr}	rear tire lateral (transversal) damping constant	
b_{lf}	front tire longitudinal damping constant	
b_{tf}	front tire lateral (transversal) damping constant	
c_r	rear tire crown radius	[m]
c_f	front tire crown radius	[m]
d_1	frame length	[m]
d_{20}	front suspension neutral length	
d_3	fork offset	[m]
d_4	swingarm length	[m]
d_r	rear tire roll radius	[m]
d_f	front tire roll radius	[m]
d_{lf}	front tire longitudinal relaxation constant	
d_{lr}	rear tire longitudinal relaxation constant	
d_{tf}	front tire lateral (transversal) relaxation constant	
d_{tr}	rear tire lateral (transversal) relaxation constant	
g	gravity constant	
k_1	rear tire vertical spring stiffness	
k_2	rear suspension vertical spring stiffness	
k_3	front suspension vertical spring stiffness	
k_4	front tire vertical spring stiffness	
m	mass	
q	generalized coordinate	
q_{70}	rear suspension neutral angle	

Contents

Chapter 1

Introduction

1.1 Background

Computer electronics is developing in a rapid pace. Processing power of personal computers has reached a state in which it is possible to simulate all kinds of interesting physical, real world, phenomena.

The advancement of computer electronics is also visible in the automotive industry. The electronics in automotive industry started with simple electronics to control engine emissions during the 70's [25], to the advanced current day's features such as power train control, vehicle motion control, airbag systems and anti-lock braking systems. Parallel to the development of these automotive electronic features, computer simulation models have been created with increasing complexity to predict the vehicle behavior. Some of these models have been implemented in vehicle onboard ECU's being part of the controller (state estimators). Future developments lead to advanced electronic systems such as fuel consumption strategies for hybrid vehicles and advanced electronics to control vehicle safety. An example of the latter is adaptive cruise control or a collision avoidance system, where the vehicle communicates with other vehicles in order to avoid a crash. The ultimate development being a fully automated vehicle that only needs a final location and will go there completely autonomous.

In the evolution of the motorcycle a similar trend can be witnessed, albeit two decades delayed. Or in other words, developments will appear two decades later in the future. The electronic evolution in motorcycles started with electronic injection systems at the end of the twentieth century, to the development of a motorcycle anti-lock braking system a few years ago. Following the automotive trends, it is expected that more of these well developed car electronic features will be used on future motorcycles [18].

1.2 Motivation

Difficulties arise when testing new electronic features on a motorcycle during the development phase, since a motorcycle is inherently unstable. One way to execute tests is to send an experienced driver out on the road and try to collect the relevant data. There are two issues with this approach. First of all, the driver itself is a controller that cannot easily be changed, so the driver will interfere with the electronics, or even adapt to the electronics. So then the question is whether the electronic device

functions as desired, or that the driver just knows how to anticipate to the electronics. Second issue is that safety critical software is hard to test and may be dangerous to test. The driver really has to go beyond the edge of motorcycle performance in order to fully test the functionality of the electronic controller. A failing controller can in that case potentially result in a severe accident.

Another way to evaluate new electronic control systems on a motorcycle is to test it on an autonomously driving motorcycle. Different driving styles could be uploaded to the motorcycle to test a controller under different circumstances and no drivers' life is at stake. Before this, the controller will be tested in a virtual environment, accurate enough to represent reality. That means the virtual environment should have a decent physics engine (in this case a driving simulator). In a simulation environment, it is easy to adapt the parameters of the autonomous motorcycle to represent different variants of the real motorcycles. Different motorcycles and different driving styles can be compared against each other in a scientific way. This kind of model with controller is not available yet. In distant future, two decades after the fully autonomous driving car has been introduced, the autonomous driving motorcycle may have its introduction to the consumer market.

1.3 Objectives

The development of a realistic motorcycle model and controller, that is needed to make the motorcycle autonomous, are the topic of this graduation project. This is because a motorcycle model with controller is not available yet. The model design is based on robot modeling, and includes a realistic tyre model, together with all the important degrees of freedom that a real motorcycle has. The model includes all gyroscopic and coriolis terms. The controller is able to follow a trajectory in the ground plane in a virtual environment, and is able to calculate the time based reference trajectory from information about its current position.

1.4 Contribution

This report describes a motorcycle model that unifies all motorcycle dynamics in one model. The model is robust since it is valid for all driving conditions of a motorcycle, and can be used for advanced simulations. The model is an addition to the current set of models that is available from literature, and has its roots in robot modeling. Advanced motorcycle models are already in use in industry, but unlike this model, they are made in multibody software packages that do not state the equations of motion in explicit form.

1.5 Outline

The 'autonomous motorcycle' consists of two parts: the motorcycle, and the drivers' substitute, from now on called the controller. Creating both motorcycle and controller in a virtual environment requires knowledge about the motorcycle dynamic behavior. Chapter 2 starts with a literature review. The literature review is divided in three topics, namely motorcycle, tyre, and driver models.

Insight in the motorcycle dynamics is not obtained by bluntly copying a motorcycle model from literature. Although many models are available from literature as a set of first order differential equations, most of them are linear, and parameters used in these models can be fairly meaningless. Therefore, Chapter 3 of this report explains the derivation of the equations of motion of a motorcycle. At the

end of Chapter 3, a second model is presented. This model has evolved from the first model, but has two more degrees of freedom, together with two constraint equations. In the last section, advantages and disadvantages of both models are discussed.

The equations of motion are programmed in MATLAB/Simulink. Programming is prone to error, so a multibody model is made with Simulink SimMechanics. The comparison of these models is part of the validation process in Chapter 4. The equations of motion are linearized in Chapter 4, and then compared with two other linear motorcycle models from literature. The nonlinear model is compared with the model made with Simulink SimMechanics, and with another nonlinear model made by W. Versteden cf. [26]. In the last part of Chapter 4, the linearized model is analyzed. The eigenvalues of steady state operating points are calculated, and plotted in the complex plane for varying camber angles.

The design of a controller is the main topic of Chapter 5. Chapter 5 starts with a discussion of several ways of controlling the motorbike. To control the bike, a certain reference trajectory has to be available. A reference trajectory is a path that should be followed by the motorcycle. The design of this virtual path is therefore the next topic of Chapter 5. Finally, the controller will be discussed.

Chapter 2

Literature review

The literature review is divided in three topics. These topics are the motorcycle model, the tyre model, and the driver model. A good starting point to learn more about motorcycle dynamics, is the book of V. Cossalter "Motorcycle Dynamics" [4]. Although this book does not explicitly cite a certain motorcycle model, it certainly provides a lot of insight in the kinematics and dynamics of motorcycles. The book explains different dynamic behavior that can be observed on a motorcycle. Each aspect is explained with a problem specific model. Furthermore, this book provides valuable rules of thumb for position of mass center, wheelbase, and other parameters of different motorcycle types such as touring motorcycles, and high performance motorcycles. Reading this book is also good to get familiar with the language terms used in motorcycle dynamics.

2.1 Motorcycle models

From a modeling point of view, simplified motorcycle models are similar to simplified bike models, and can be used to represent either of the two. Therefore, bikes and motorcycles are treated as the same. Many models describing bike and motorcycle dynamics can be found in literature today. The simplest models that can still reveal some of the dynamics are second order. Examples of these models are [27], [7] and [3]. These models stem from the beginning of the twentieth century. They describe the motorcycle lean angle and lean angular velocity as a function of the steer angle. These models are mainly concerned about the instability observed in bicycles and try to explain why a rolling bike is stable in it's upright position. These models are very simplistic and cannot be used for a realistic dynamic motion simulation. These models also do not predict a self-stabilizing velocity region for the motorcycle. A picture of a simple bicycle model is drawn in Figure 2.1, [27].

As the reason for upright stability was still a debate, different models are derived with different terms omitted or included. Examples of these terms are inertia of the front frame, angular momentum of the wheels and different terms that should represent the trail distance [15]. The terms of some of these models are nonlinear. As time progresses, the order of these models increases as well. In the first half of the twentieth century, the investigation of the stability of bikes lead to ever more complex mathematical descriptions of bikes. A good example is the work of Döhring [6]. The description of Döhring is complex and accurate [15]. However, in that time there was no possibility to evaluate the equations of motion, since there was no computer available.

After Döhrings' work, people like Koenen [12] also derived the motorcycle dynamic equations by

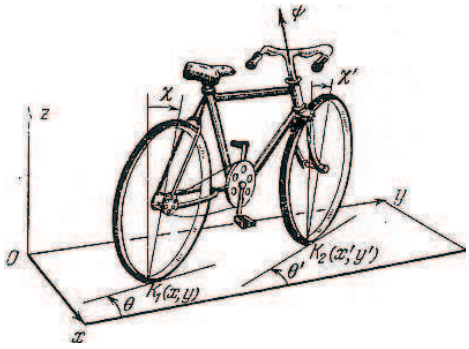

Figure 2.1: simple bicycle model [27].

hand. The difference is that they could subsequently implement the equations in a computer to evaluate and investigate the dynamic response. References [12] and [20] are more concerned with motorcycle performance than stability and include more details in their motorcycle model than most other bike models at that time. The equations include the suspension and forward motion, as well as frame compliance and tyre dynamics. The model of Koenen [12] is 28th order and has an advanced tyre model included, that is still in use today. However, the derivation is done completely by hand and [15] discovered some minor errors. The work of W. Versteden [26] builds on the work of Koenen. It has the model of Koenen implemented in a multibody software package and the different motorcycle tyre model parameters are measured.

With the diffusion of computers also more advanced software packages arise, that make hand calculations old fashion. With model based simulation an almost unlimited number of degrees of freedom can be used. Software packages can nowadays predict the motorcycle motion without explicitly requiring the equations of motion. Although the motion itself may be sufficient, the equations of motion give more insight in the motorcycle behavior. With an ever increasing complexity of models, also the number of parameters increases. These parameters have to be estimated and inaccurate parameters can lead to an inaccurate model. A good balance between model complexity and number of model parameters is therefore important. As stated in [15], from that date (june 2007) there is yet no consensus that any peer-reviewed paper in English has the correct equations. Multibody software models may seem to be correct but they can not be rigourously proven to be correct. Besides that, the information enclosed in a multibody software model is only available to a small group of people. A paper like [22], that pretends to explain the model, cannot be used to actually build the model.

A literature study reveals that different models require different sets of parameters. This has a large impact on the model size, but also on ease of measurement. Some variable definitions are easier to measure on a real bike than others. Another thing to mention is that the order of a bike model varies between two and almost infinite. The choice of the number of degrees of freedom is important since it defines which physical phenomena can be simulated and which not. The complex multibody models with a high complexity and a large number of degrees of freedom are not available for general public. Building a model in a simulation environment is easy, but finding the accurate values for the parameters and validating the model is difficult. A new model that has not been validated thoroughly will not be accepted in the scientific community. Furthermore, highly complex models do not give insight in the equations of motion and are thus difficult to use for controller development purposes. Therefore, large and complex models are inconvenient to use in this graduation project. In this project the minimal number of degrees of freedom are sought that can still predict the position of the motorcycle in three dimensional space as a function of time. A two degree of freedom motorcycle model is too simple to be used for control purposes. To be able to control the position of the motorcycle, at least 6 degrees of freedom (DOF) are needed, namely the position and orientation of the motorcycle as a rigid object in three dimensional space. These six DOFs do not say anything about the dynamics

of the motorcycle as a multibody system. Reference [4] summarizes the most important degrees of freedom in a motorcycle to be the rotation of the handlebar, the suspension and the rotation of the wheels. Together this adds up to 11 DOF. The absolute minimum would be 7, being the 6 DOF in 3D space and the steering of the handlebar. This number of DOF however, is not able to predict bounce or hop and cannot be used to include an advanced tyre model. Also it is not possible to determine longitudinal slip.

2.2 Tyre models

The tyre is probably the single most important component of the motorcycle, which defines the largest part of the motorcycle dynamic behavior. This is due to the tyre being the only component that delivers desired interaction forces with the environment of the motorcycle. Several mathematical tyre models have been developed in the twentieth century. These models range from mainly theoretical descriptions to empirically derived descriptions. The goal of every model is to represent the tyre dynamic behavior accurate. The bike models developed at the beginning of the twentieth century did not include a tyre model at all and treated the tyre as a simple kinematic constraint. For example in Reference [9], the wheel in this model is a body fixed to the rear frame that is able to move in longitudinal direction, and not in lateral direction. Vertical motion of the wheel is also restricted with a constraint on position level. Rolling of the wheel is not included in this model. The Whipple model [27] treats the tyres as rigid, two dimensional rolling disks having a separate mass and inertia. This allows for gyroscopic forces. The rolling is restricted with a nonholonomic constraint that is known in literature as the pure rolling constraint. The equations of motion resulting from this description are similar to the mathematical Euler disk equations of motion [24].

Advanced tyre models are able to slip in longitudinal direction, as well as sideways. These models use the slip and camber angle in the contact patch between the tyre and the road in order to generate a force. Tyre contact patch force is not a fundamental force such as gravity, electromagnetic force, or nuclear force. Instead, tyre force is believed to be a result of microscopic electromagnetical force. Therefore the force as a function of slip assumption is justified. The most important tyre model used in industry today is the TNO-Delft tyre. Another tyre model that is sometimes used is the University of Arizona tyre model [5]. Except for some minor slip definitions, both tyre models are basically the same. The approach in the TNO-Delft tyre is empirical and the results reproduce the measured behavior of a real tire very well.

2.3 Driver models

The final topic that has been studied from literature are the controllers used for bicycles. Soon after models of bikes were created, people realized that the riderless bike or motorcycle is unstable in almost all steady-state operating points. In some literature models, the controller is part of the bike [8]. The most common controller is a proportional and differential feedback from the bike inclination angle to the bike steering angle. It is interesting to note that for a long time, people were only concerned about stabilizing the bike and not on path tracking control problems. It is like a person knowing how to stabilize the bike, without being able to go anywhere. With the need to track a certain reference trajectory in the ground plane comes the need to include the position and heading of the motorcycle into the set of generalized coordinates. Even as late as 2009 [10], position and heading were neglected, and interest was only in stabilizing the electric bicycle. Few articles are devoted to trajectory tracking, and the first articles only appears in the last decade of the twentieth century.

An interesting article appeared in 2006 about an unmanned motorcycle participating in the DARPA challenge [28]. In this article, Jingang also underlines the lack of literature about trajectory tracking. In their article, they describe a simplified bike model comparable to the Whipple model. The position is subsequently derived from the velocity, which in turn is derived from the yaw angle. The bike model is simple, but the model allows for trajectory planning. The controller is based on input output feedback control where the input is from a GPS signal and a digital camera. Tanaka and Murakami also use a (PD) controller to stabilize a bicycle [21]. The bike model they use is a simplified inverted pendulum model for bicycle balancing. Balancing is the main concern and trajectory tracking control is not discussed in [21]. Controllers that use more elaborate motorcycle models are made by R. Sharp in [19] and also separately by Kessler in [11]. Both [19] and [11] make use of a dynamics simulation package. In [19], Robin Sharp explains results of a model of the real driver including lean. The focus is not on the control, but on the motorcycle rider combination. Kessler uses a multibody model made with ADAMS. The model seems to be fairly complex, but the controller is a simple feedback of yaw, which is measured with a gyroscope, and forward velocity. The motorcycle inclination is not used, which makes stabilizing impossible as is also shown in this thesis. Both [19] and [11] use a complex motorcycle model in a software environment. This model is not discussed with enough detail to recreate it. Although it is believed that these models are fairly accurate, otherwise they are meaningless for the ones that have no acces to it.

2.4 Summary

The number of bike models seem to explode since the digital revolution. Anyone can make a model in a multibody modeling environment. Some people are interested in analyzing the dynamics of motorcycles and use fairly complex models. Other groups are mainly interested in controlling the bike and tend to use a more simplistic model. People realized that a benchmark should be defined in order to compare all these models [1]. Several summaries of motorcycle and bicycle models can be found in literature. Besides [1], good bicycle and motorcycle model summaries are given in [17], [13], and [4]. Designing a motorcycle controller could be done with an advanced model. With an advanced model, boundaries of motorcycle performance can be sought. For a control engineer, it can be hard to interpret these advanced models. Therefore, a good explanation of a complex model should be given. There has not been a single article that explains the used model with enough detail, so that it can be implemented by a third party. A control engineer likes to use a model as a tool that he is confident with. Therefore, this report explains an advanced motorcycle model that can be used for reference trajectory tracking control purposes. Therefore, the derivation of a motorcycle model is explained in the following chapter.

Chapter 3

11 DOF motorcycle model

In this chapter, an eleven degrees of freedom motorcycle model is derived. The emphasis of this chapter is not on the model itself, but on the derivation of the equations of motion for this model. It is believed that, if the reader can follow the derivation, the model will be accepted and used more easily. Section 3.1 is an introduction to the model. It is the backbone of the model and discusses the general equations of motion to see which ingredients are needed to derive these equations of motion. The section reveals that the generalized coordinates, model parameters, and position vectors are needed for deriving the equations of motion. The position vectors of the individual bodies should be derived as a mathematical function of the generalized coordinates and motorcycle parameters. Therefore, this chapter starts in Section 3.2 with the description of the main components of the motorcycle. The model consists of six separate bodies. The choice and number of bodies is discussed in Section 3.2. Next, the choice of parameters and the generalized coordinates used to describe the model are explained. With these ingredients, the position vectors needed for the equations of motion of the motorcycle model can be formulated. This is done in Section 3.3. Next, the forces acting on the system are stated and expressions for these forces are given in Section 3.4. With the forces given, the equations of motion can be completed in Section 3.5. Finally, in appendix D, a second approach is given. The advantages and disadvantages of both models are discussed in appendix D.1.

3.1 Model architecture

The motorcycle model is a set of eleven second order differential equations. These equations are derived from classical mechanics and describe the motion of the motorcycle as a function of the forces acting on the separate bodies of the motorcycle. Therefore, these equations are also called the equations of motion. The basis of the motorcycle equations of motion are the Euler-Lagrange equations. The Euler-Lagrange equations can be stated as;

$$M(q) \cdot \ddot{q} + C(q, \dot{q}) \cdot \dot{q} + P(q) = W(q, \dot{q}) \tag{3.1}$$

In (3.1), q is a column of eleven independent, also called generalized, coordinates. These coordinates are variables that can have any value, independent of each other. The first derivative with respect to time of the generalized coordinates is $\dot{q}$, and the generalized coordinates' second derivative with respect to time equals $\ddot{q}$. Vectors $\dot{q}$ and $\ddot{q}$ are called generalized velocities and generalized accelerations respectively. The meaning of $M(q)$, $C(q, \dot{q})$ and $W(q, \dot{q})$ is explained in the following paragraphs. The equations of motion in this form comes from robot modeling, and is elaborated in detail in the book 'Robot Modeling and Control', [14]. In [14] the term $C(q, \dot{q})$ is called $D(q, \dot{q})$, which is incon-

venient since D is also used as a direct feedthrough term in state space representation. Therefore, the naming of [23] has been used in this case. In the following paragraphs, more of these minor differences have been used, but naming is always similar to one of Spong [14], Wouw [23], or Kraker [2].

Acceleration term

The first term on the left side of (3.1) is the only term containing generalized accelerations. The matrix $M(q)$ is the dynamic mass matrix and is a function of the generalized positions and the motorcycle parameters. Because the model doesn't contain any transport kinetic energy and mutual kinetic energy terms, the mass matrix can be formulated as;

$$M\left(q\right) = \sum_{i=1}^{n} \frac{m_i}{2} \left(\frac{\partial O_i}{\partial q}\right)^T \frac{\partial O_i}{\partial q} + \sum_{i=1}^{n} \sum_{j=1}^{3} \left(\frac{I_{ji}}{2} \omega_{ji}^T \omega_{ji}\right) \tag{3.2}$$

In (3.2), there are two terms: the first term sums the translational kinetic energy of all bodies, and the second term over the rotational kinetic energy of all bodies. Therefore, the index n in (3.2) equals six, because the motorcycle is divided in six separate bodies, as will be explained in Section 3.2. These six bodies are also summarized in table 3.1. The mass of body i is m_i,and O_i is the position of the center of mass of body i. The rotational inertia of body i around the j^{th} axis of the inertial reference frame equals I_{ji}, and ω_{ji} is the angular velocity of the i^{th} body around the j^{th} axis of the inertial reference frame. They (I_{ji} and ω_{ji}) can be calculated as,

$$\begin{aligned}
I_{1i} &= \tfrac{1}{2}\left(I_{yi} + I_{zi} - I_{xi}\right), & \omega_{1i} &= \tfrac{\partial}{\partial q}\left(R_i \cdot \left[\begin{smallmatrix} \mathrm{I} \\ \mathrm{o} \\ \mathrm{o} \end{smallmatrix}\right]\right), \\
I_{2i} &= \tfrac{1}{2}\left(I_{xi} + I_{zi} - I_{yi}\right), & \omega_{2i} &= \tfrac{\partial}{\partial q}\left(R_i \cdot \left[\begin{smallmatrix} \mathrm{o} \\ \mathrm{I} \\ \mathrm{o} \end{smallmatrix}\right]\right), \\
I_{3i} &= \tfrac{1}{2}\left(I_{xi} + I_{yi} - I_{zi}\right), & \omega_{3i} &= \tfrac{\partial}{\partial q}\left(R_i \cdot \left[\begin{smallmatrix} \mathrm{o} \\ \mathrm{o} \\ \mathrm{I} \end{smallmatrix}\right]\right).
\end{aligned} \tag{3.3}$$

In (3.3), R_i is the rotation matrix that maps the vectors of the inertial reference frame to the local orientation of body i. I_{xi} Is the inertia around the body's local x-axis, I_{yi} is the inertia around the body's local y-axis, and I_{zi} is the inertia around the body's local z-axis. The body's local x-, y-, and z-axis are the principal axes of the body.

Velocity term

The second term on the left side in Equation 3.1 arises from differentiating the kinetic energy towards the generalized coordinates and generalized velocities. $C\left(q, \dot{q}\right)$ is an 11 by 11 matrix containing the contribution of the centrifugal and coriolis forces to the equations of motion. In literature, $C\left(q, \dot{q}\right)$ is called the Christoffel matrix. The Christoffel matrix can be calculated from the mass matrix.

$$C_{kj}\left(q, \dot{q}\right) = \sum_{i=1}^{11} \frac{1}{2} \left(\frac{\partial M_{kj}}{\partial q_i} + \frac{\partial M_{ki}}{\partial q_j} - \frac{\partial M_{ij}}{\partial q_k}\right) \cdot \dot{q}_i \tag{3.4}$$

The subscripts i, j and k in (3.4) refer to the mass matrix entry respectively the column of generalized coordinates entry, not to be confused with the meaning of the subscripts in (3.2) and (3.3).

Gravitational term

The third term on the left side of (3.1) arises from potential energy stored in the system due to the fact that the system is located in the earth's gravitation field. Other forms of potential energy could have been added to this term. For example, the front and rear suspension force can be separated in two parts; the conservative part that forms the recoverable, elastic, internal energy (spring) and the nonconservative, dissipative part (damper). The nonconservative part is then placed on the right side of Equation 3.1 inside $W(q, \dot{q})$. However, since the nonconservative part of the force must be placed inside $W(q, \dot{q})$, it is easier to place both the conservative and non-conservative force inside $W(q, \dot{q})$. The potential energy due to the earths gravity field can be calculated as

$$P(q) = \sum_{i=1}^{6} \frac{\partial O_i}{\partial q} \cdot \mathbf{g} \cdot m_i \tag{3.5}$$

In (3.5), $\mathbf{g}$ is the gravity vector, which is given as $\begin{bmatrix} 0 & 0 & -g \end{bmatrix}^T$.

Force term

As stated in the previous paragraph, the last part of Equation 3.1 consists of all applied forces minus the internal forces. Internal forces are forces inside the system, that do not deliver work. This term is called the external force ter, and is a form of virtual work done by all external forces. The virtual work done by the external forces can be calculated as

$$W(q, \dot{q}) = \sum_{i=1}^{m} \frac{\partial O_i}{\partial q}^T \cdot F_i + \sum_{i=1}^{n} \frac{\partial}{\partial q}^T \cdot T_i \tag{3.6}$$

The virtual work term, $W(q, \dot{q})$, is a sum of seven (m=7) applied forces (F_i) and nine (n=9) applied torques (T_i). Two torques and three forces are acting on each wheel. The front suspension is treated as an applied force, and the rear suspension is handled as an applied torque. Furthermore, there are another four torques that can be used as control variable. These four torques are the front and rear brake torque, the engine torque, and the steering torque. A more detailed discussion about the forces and torques is given in Section 3.4, where the forces and torques are elaborated further.

From the previous discussion, it is clear that to obtain the equations of motion for the motorcycle, one has to distinguish between the separate bodies and develop expressions for the position and orientation of each body. Since the position and orientation of each body is dependent on the generalized coordinates (q) and motorcycle parameters, these have to be defined first. Therefore, Section 3.2 starts with a discussion of the individual bodies, followed by the explanation of the parameters and generalized coordinates. After that, in Section 3.4, the external forces and torques are explained in detail.

3.2 Bodies of the motorcycle

As already mentioned in the previous section, the motorcycle is modeled as six rigid bodies. These rigid bodies are summarized in table 3.1. Some comments can be made on the choice of the separate bodies.

The most important object is the main body. It contains the largest part of all mass. The engine, transmission, fuel tank, frame and seat are all parts of the main body. One could argue that the dynamic behavior of the swingarm could be neglected compared to all dynamics inside the main body. However, there are several reasons why the swingarm has been separated from the main body.

First, by considering the swingarm and the front fork as separate bodies, there is a clear distinction between sprung and unsprung mass. The vertical dynamics can thus be united with lateral dynamics, which is important for transient cornering dynamics at large forward velocity and a sharp turn radius.

Second, the parts in the current division form a path starting at the rear wheel and ending at the front wheel. Expanding the model by separation of the main body into smaller bodies, for example if there is an interest in finding high frequency dynamics occurring from the internals of the main body, then it is easy to expand the current model, since the newly defined bodies are not part of this chain, but can be added on top of the main body.

Finally, the dynamics of the separate parts have comparable timescales, each having a clear contribution to the overall dynamics of the motorcycle. For example dynamics of the valve train are supposed to be very high frequent. Simulating these dynamics wil need very small time steps, while the interest is more on the global motion and in the lower frequency dynamics. It might be better to model these dynamics as noise, or as a disturbance force term. These dynamics are neglected in this report and not considered, since it will not severely influence the overal dynamics of the motorcycle.

The driver is also not included in the model since it is not part of the motorcycle. The driver is not a rigid object and the motion that is executed by the driver is unpredictable and uncontrollable. Also, the aim is to develop an autonomous motorcycle for testing extreme riding conditions with no driver.

Table 3.1: motorcycle parts

Object	Name
1	rear wheel
2	swingarm
3	main body
4	steering head
5	front fork
6	front wheel

It is clear from (3.1) to (3.6), that the position vectors of these bodies should be written as a function of the generalized coordinates q. To do that, the set of generalized coordinates should be defined first. This is done in the next section.

generalized coordinates

The motorcycle model has eleven degrees of freedom (DOF). These are defined as follows. The motorcycle as an object in three dimensional space has six degrees of freedom; three translational, and three rotational degrees of freedom. On top of these six DOFs, there are two DOFs for the front and rear suspension deflection, two DOFs for the rotation of the wheels and one DOF for the steering axis. Together, this adds up to eleven DOFs. Eleven DOFs means that eleven generalized coordinates have to be defined. In the process of deriving the model equations, several iteration steps have led to different sets of generalized coordinates. The set of generalized coordinates presented here result in a compact formulation with the smallest number of logic operations in the equations. Each generalized

coordinate has been given a name so that it is easy to refer to a certain coordinate. The coordinates and their names are summarized in Table 3.2. The order in which the generalized coordinates are stored in the column q is the same as in Table 3.2. The generalized coordinates will be explained next.

Table 3.2: Generalized coordinates

Name	Short description	Units
$q(1) = x_0$	x-coordinate	[m]
$q(2) = y_0$	y-coordinate	[m]
$q(3) = z_0$	z-coordinate	[m]
$q(4) = q_0$	yaw angle	[rad]
$q(5) = q_1$	camber angle	[rad]
$q(6) = q_2$	pitch angle	[rad]
$q(7) = q_3$	steer angle	[rad]
$q(8) = q_6$	swingarm angle	[rad]
$q(9) = d_2$	fork length	[m]
$q(10) = q_9$	rear wheel orientation	[rad]
$q(11) = q_{10}$	front wheel orientation	[rad]

x_0, y_0, z_0; x-coordinate, y-coordinate, z-coordinate

The first three generalized coordinates are translational. These coordinates give the motorcycle the freedom to translate. The x-, and y-coordinate are not the same as the lateral and longitudinal direction of the motorcycle. The x-, y-, and z-coordinate together form a vector, that defines the position of the joint between the main frame and the steering head. This point is defined in a three dimensional space measured w.r.t. an inertial reference frame that is fixed to earth and it is independent of any coordinate system internal to the motorcycle.

q_0; yaw

Yaw is the vertical orientation of the main body of the motorcycle. It is the angle between the x-axis of the global reference frame and the line of intersection of the ground plane with the plane of symmetry of the motorcycle. The rear wheel and the swingarm and the main body will experience the same yaw angle. Note that the yaw is always a rotation around an axis perpendicular to the plane spanned by the x-coordinate and y-coordinate. That is, no matter if the bike is standing straight, or laying on its side. Yaw maps the x coordinate of the global reference frame to the longitudinal coordinate of the motorbike. The yaw coordinate is visualized in figure 3.1.

q_1; frame camber

The frame inclination angle is the camber of the main body. Therefore, it is also the inclination of the motorbike rear wheel and swingarm. In other papers, this coordinate is sometimes called roll. Roll however, might be confused with the rolling of the wheels. Inclination is the angle that maps the absolute vertical axis to the motorbike vertical axis. This is also visualized in figure 3.2.

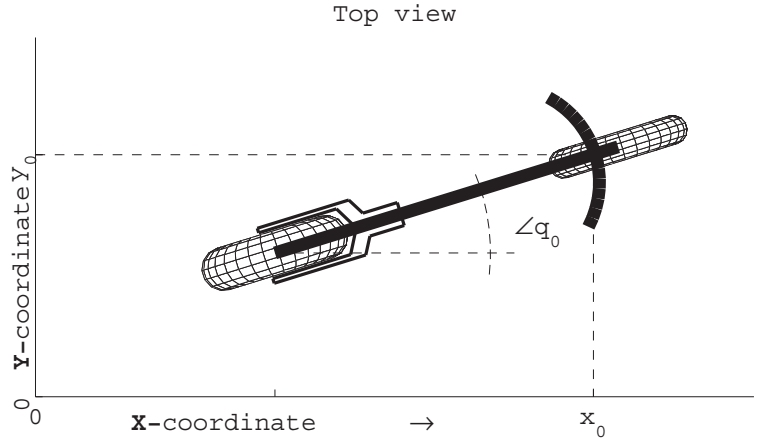

Figure 3.1: Definition of the yaw, q_0.

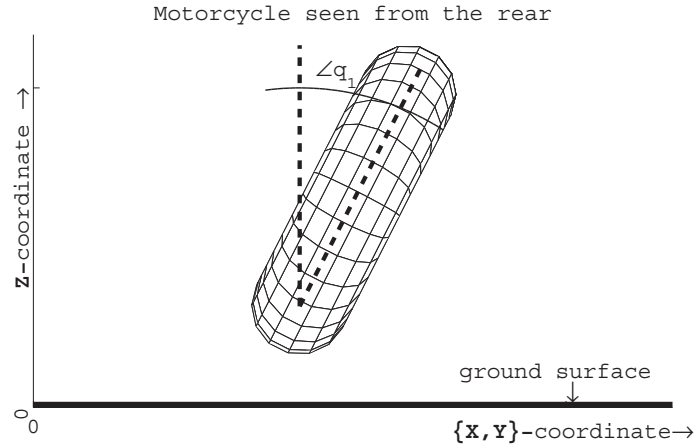

Figure 3.2: Definition of the rear camber, q_1.

q_2; pitch

Pitch is the toughest generalized coordinate to explain. Although the word in itself covers its meaning very well, giving a clear definition appears to be difficult. In a lot of texts about the subject, pitch is given as the angle between the horizontal ground plane and a vector fixed to the motorcycle laying in the plane of symmetry of the motorcycle. This definition is not accurate enough. It is in conflict with the definition of camber. The issue is that the order is important. In the aforementioned definition, it may be unclear what came first: camber or pitch? Another definition, that circumvents this order problem is to say that pitch is the rotation around an axis perpendicular to the motorcycle plane of symmetry that is needed to keep the front wheel on the ground surface. In the current model however, this is not true because that would mean that the pitch is a function of all other coordinates together with the motorcycle dimensions. That cannot be true because pitch will not be an independent coordinate anymore. The best way to define this coordinate is to imagine a rotation around an axis perpendicular to the motorcycle plane of symmetry, that is there to give the motorcycle main body it's final degree of freedom to allow it to obtain any orientation in space. Note that when the camber is 90 degrees, pitch coincides with yaw and gimbal lock occurs. Gimbal lock is not observed in reality off course, because a bike on its side can still rotate around a horizontal axis that is the vertical axis of the motorcycle. Fortunately, a camber angle of 90 degrees in normal operating conditions is very

rare [1]. Simulation of the model is aborted when the absolute value of the frame camber exceeds 80 degrees. Pitch is visualized in figure 3.3

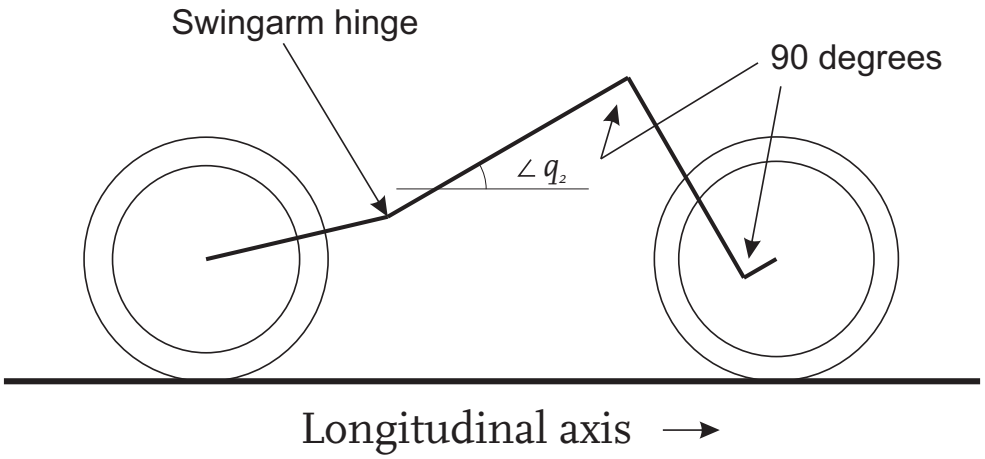

Figure 3.3: Definition of the pitch, q_2.

q_3; Steering angle

The steering angle is the relative angle between the motorcycle main body and the steering head. This angle is measured perpendicular to the steering axis. A positive steering angle is a rotation to the left.

q_6, d_2; Swingarm angle and front suspension

The coordinate q_6 is a rotation to map from the fixed world directly to the pitch angle of the swingarm. It has a similar meaning as the pitch angle q_2 for the main body, but then for the swingarm. This coordinate allows the swingarm to move with respect to the frame. The front suspension translational degree of freedom is d_2. The character (d_2) originates from the basic bicycle model in literature. The name (d_2) makes sense in the light of the important motorcycle dimensional parameters, which are described in figure 3.5 and in the next section. The coordinates q_6 and d_2 are important because they describe the relative motions of the wheel centre w.r.t. the frame.

q_9, q_{10}; Rotation of the rear and front wheel

The coordinates q_9 and q_{10} are the rotation of the rear and front wheel respectively. These coordinates are added to include longitudinal slip from the tire model. The tire model calculates forces on the tire that are caused by velocity differences between the road and the tire contact patch. q_9 and q_{10} also have a similar meaning as the pitch angle q_2 for the main body, but then for the wheel bodies. These angles are again absolute angles.

[1] from the definition of q_1, camber angle is the angle between the tire vertical plane and the absolute vertical plane. this means that on banked corners, it is possible to have a camber angle of 90 degrees or more

dependent coordinates

In the model, it is sometimes convenient to go from one orientation to the other without using all the intermediate coordinates. These derived coordinates are an easy way to short cut transformations. For example, the camber angle of the front wheel (q_5) can be expressed in the generalized coordinates q_1, q_2 and q_3. If this expression is derived, one can just use q_5 instead of the complex expression using q_1,q_2 and q_3 as the notation.

q_7; swingarm deflection angle

The swingarm deflection angle q_7 is the angle between the swingarm and the main body of the motorcycle. In an early version of the model, this was a generalized coordinate. For mathematical simplification reasons, this coordinate has been depreciated to a derived coordinate and the absolute angle q_6 is used as a generalized coordinate instead. The coordinate q_6 can be seen as a rotation to map from the fixed world directly to the swingarm rotation. In the previous section, it was explained that q_7 is a relative rotation (relative w.r.t the main body). The pitch, q_2, is the absolute rotation of the main body. This mean that the rotation of the swingarm w.r.t. the main body can be written as:

$$q_7 = q_2 - q_6 \tag{3.7}$$

q_4; front fork plane pitch

The front wheel plane pitch is the pitch measured in the front wheel plane. This frame is created by subsequently adding yaw, camber, pitch and steer when starting at the inertial reference frame. To get the frame back to its original orientation, one can first extract the steer, then the frame pitch, then the camber, and finally the yaw. Another way to transform the frame back to the inertial reference frame is to first rotate the reference frame around the pitch axis over an angle q_4 such that one vector of the frame is parallel to the ground. From this, q_4 should be such that the inner product of the absolute vertical with this vector should be zero.

$$q_4 = -\arctan\left(\frac{\sin(q_2)\cos(q_3) - \tan(q_1)\sin(q_3)}{\cos(q_2)}\right) \tag{3.8}$$

q_5; front wheel camber

The camber of the front wheel denoted by q_5. This is the angle between a vector that is perpendicular to the steering axis and front wheel rolling direction, and the ground plane. It is the angle between the wheel plane of symmetry and the line normal to the road plane. It is a function of q_1,q_2 and q_3. This function is as follows:

$$q_5 = -\arcsin(\cos(q_1)\sin(q_2)\sin(q_3) + \sin(q_1)\cos(q_3)) \tag{3.9}$$

q_8; kinematic steering angle

The steering angle q_3 projected on the ground surface is called the kinematic steering angle. This angle, measured in the ground plane, is a function of the generalized coordinates q_1, q_2 and q_3. This

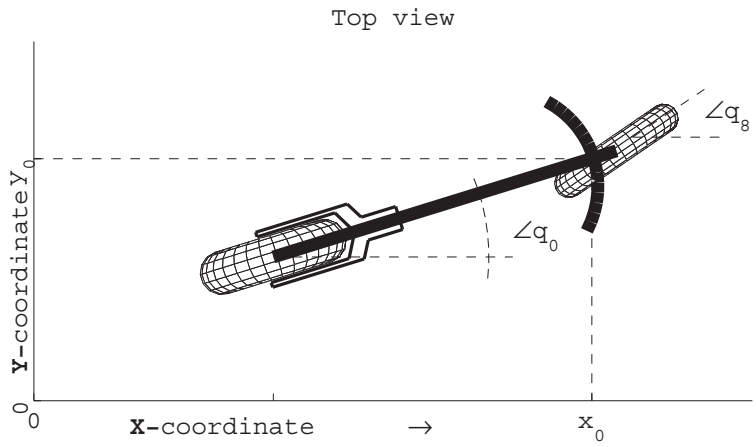

Figure 3.4: Definition of the kinematic steering angle, q_8.

coordinate is also pictured in Figure 3.4.

$$q_8 = q_0 + \arctan\left(\frac{\cos(q_2)\sin(q_3)}{-\sin(q1)\sin(q_2)\sin(q_3) + \cos(q_1)\cos(q_3)}\right) \tag{3.10}$$

The derived coordinates can easily be constructed with the aid of rotation matrices. Rotation matrices are explained in Section 3.3.

parameters

The motorcycle model uses parameters that can be subdivided in three groups, namely:

- kinematic parameters
- inertia parameters
- force parameters

Table 3.3: kinematic parameters

Name	Short description	Units
d_1	frame length	[m]
d_3	fork offset	[m]
d_4	swingarm length	[m]
d_r	rear tire roll radius	[m]
d_f	front tire roll radius	[m]
c_r	rear tire crown radius	[m]
c_f	front tire crown radius	[m]
b_r	$d_r - c_r$	[m]
b_f	$d_f - c_f$	[m]

The kinematic parameters are used to describe the main geometrical dimensions of the motorbike and the wheels. These parameters are used to describe the position of the joints and rotation points. The positions of the joints are given in motorcycle dimensions that are relatively easy to measure. The parameters that are used to describe the position of the joints in the motorcycle are visualized in Figure 3.5. Geometrical properties and rotation points of the wheels are visualized in Figure 3.6. The kinematic parameters are sufficient for the visualization of the motorcycle model.

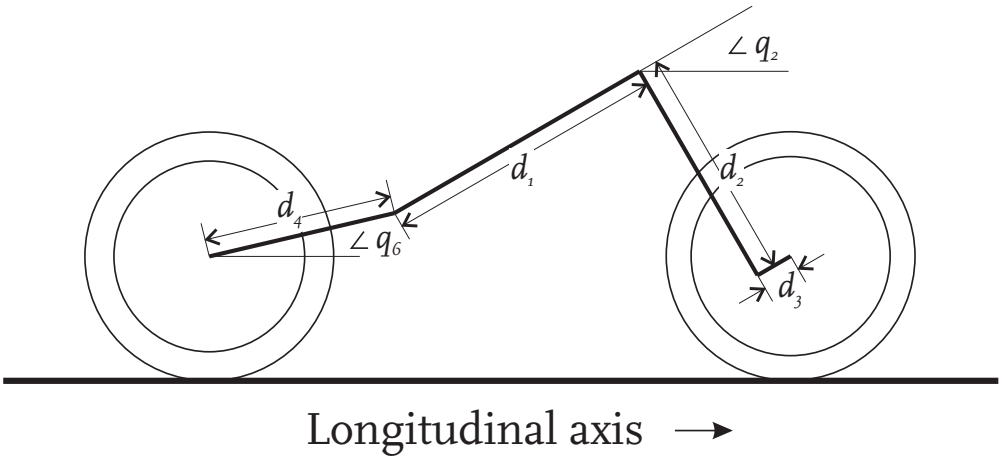

Figure 3.5: kinematic parameters.

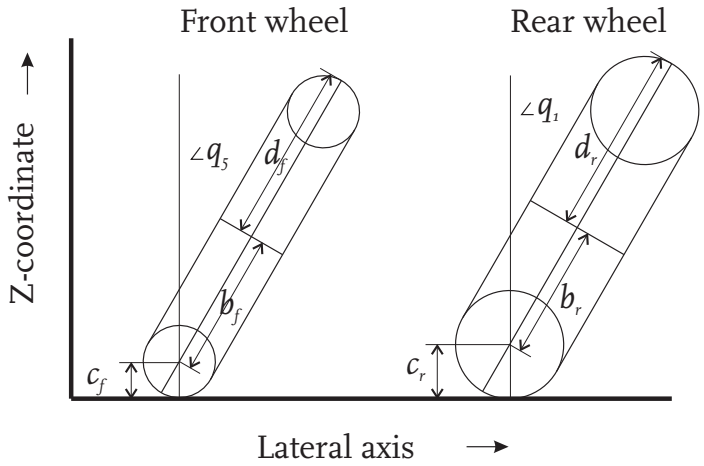

Figure 3.6: parameters referring to the wheel geometry.

Dynamic parameters relate to the mass and inertia properties of the different bodies within the motorcycle. There are four basic parameters for each body. They are the mass (m_i), the inertia (I_i), the position relative to its nearest joint and the orientation relative to the orientation of the nearest joint. The parameters that position the mass centers are visualized in figure 3.7. The center of mass position can be negative as well as positive. For the wheels, the mass center position is exactly the same as the position of the wheel centre. In Figure 3.7, the parameters p_{iq}, where i refers to body i, are the rotations of the joint coordinate systems towards the principal axes of the body. Note that the principal y-axis of each body is thus always in lateral direction. Also, the principal x- and z- axis of the wheels

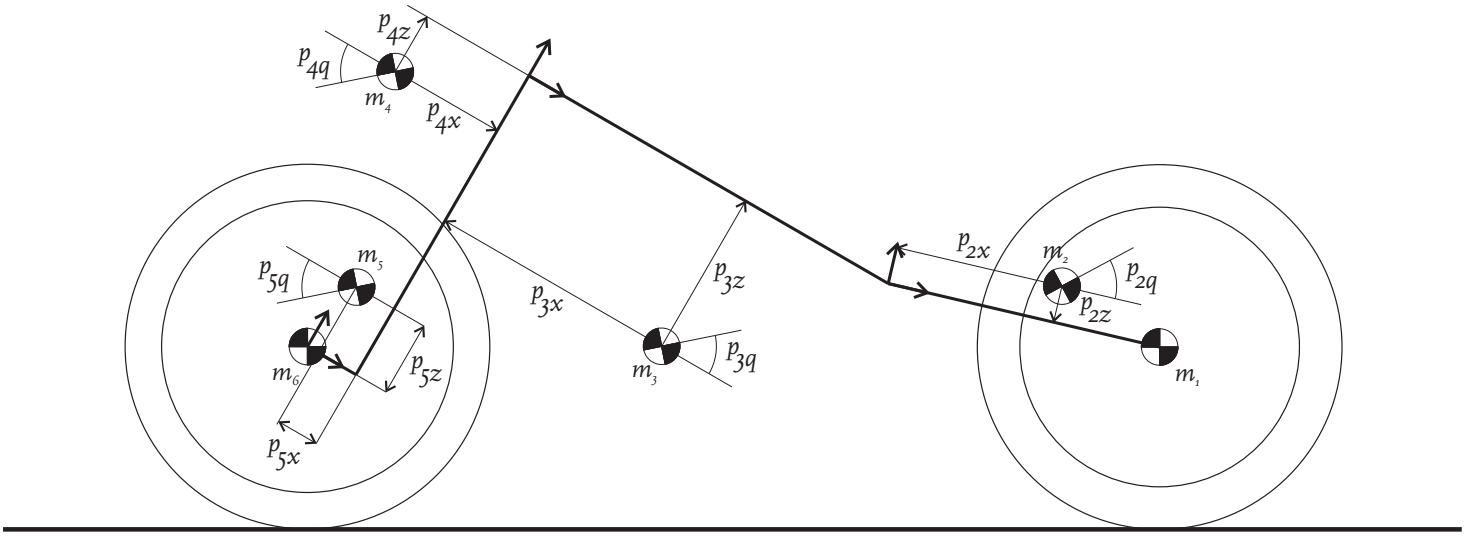

Figure 3.7: parameters describing the center of mass position relative to the nearest joint.

are equal. The center of masses are assumed to lie exactly in plane with the joints, and therefore, p_{iy} also doesn't exist (again, i is the body number).

Force parameters describe characteristics like spring constant or tire stiffness. They are used in the formulation of the forces. Force parameters cannot be visualized in a figure, but are summarized in table 3.4. The force parameters will be further discussed in Section 3.4, where the forces acting on the system are explained.

This section discusses the generalized coordinates and the parameters that are needed to write down the position and orientation of the joints and mass centers. The ingredients to formulate the position vectors and orientation matrices needed for the equations of motion are now available. Therefor in the next section, Section 3.3, an expression for these vectors and matrices is given.

3.3 Orientation matrices and position vectors

In this section, expressions for particular points inside the motorcycle are given. Because a point inside the motorcycle is given by its x-, y- and z- coordinates with respect to the inertial reference axis, the expression for a point in the motorcycle is given by a vector equation. Rotation of a vector is easiest described with rotation matrices. To rotate a vector, it only has to be pre-multiplied with the right rotation matrix. Therefore, this section starts with the definition of the rotation matrices that are used in the expressions for the positions. The rotation matrices contain sine and cosine functions. For convenience, the sine of q_i is denoted as s_i, and the cosine of q_i is denoted by c_i.

$$s_i = \sin(q_i), \qquad c_i = \cos(q_i) \tag{3.11}$$

Table 3.4: force parameters

Name	Short description
g	gravity constant
q_{70}	rear suspension neutral angle
d_{20}	front suspension neutral length
k_1	rear tire vertical spring stiffness
k_2	rear suspension vertical spring stiffness
k_3	front suspension vertical spring stiffness
k_4	front tire vertical spring stiffness
b_1	rear tire vertical damping constant
b_2	rear suspension vertical damping constant
b_3	front suspension vertical damping constant
b_4	front tire vertical damping constant
b_{lr}	rear tire longitudinal damping constant
b_{tr}	rear tire lateral (transversal) damping constant
b_{lf}	front tire longitudinal damping constant
b_{tf}	front tire lateral (transversal) damping constant
d_{lr}	rear tire longitudinal relaxation constant
d_{tr}	rear tire lateral (transversal) relaxation constant
d_{lf}	front tire longitudinal relaxation constant
d_{tf}	front tire lateral (transversal) relaxation constant

Table 3.5: dynamic parameters and mass position

Name	Short description	Units
m_i	mass of object i	[m]
I_i	Inertia matrix of object i measured in mass center	[m]
$\mathbf{p_i}$	position vector pointing from the nearest joint to the mass center	[m]

$$R_0 = \begin{bmatrix} c_0 & -s_0 & 0 \\ s_0 & c_0 & 0 \\ 0 & 0 & 1 \end{bmatrix} \quad R_1 = \begin{bmatrix} 1 & 0 & 0 \\ 0 & c_1 & -s_1 \\ 0 & s_1 & c_1 \end{bmatrix} \quad R_2 = \begin{bmatrix} c_2 & 0 & s_2 \\ 0 & 1 & 0 \\ -s_2 & 0 & c_2 \end{bmatrix}$$

$$R_3 = \begin{bmatrix} c_3 & -s_3 & 0 \\ s_3 & c_3 & 0 \\ 0 & 0 & 1 \end{bmatrix} \quad R_4 = \begin{bmatrix} c_4 & 0 & s_4 \\ 0 & 1 & 0 \\ -s_4 & 0 & c_4 \end{bmatrix} \quad R_5 = \begin{bmatrix} 1 & 0 & 0 \\ 0 & c_5 & -s_5 \\ 0 & s_5 & c_5 \end{bmatrix}$$

$$R_6 = \begin{bmatrix} c_6 & 0 & s_6 \\ 0 & 1 & 0 \\ -s_6 & 0 & c_6 \end{bmatrix} \quad R_8 = \begin{bmatrix} c_8 & -s_8 & 0 \\ s_8 & c_8 & 0 \\ 0 & 0 & 1 \end{bmatrix} \quad R_9 = \begin{bmatrix} c_9 & 0 & s_9 \\ 0 & 1 & 0 \\ -s_9 & 0 & c_9 \end{bmatrix}$$

$$R_{10} = \begin{bmatrix} c_{10} & 0 & s_{10} \\ 0 & 1 & 0 \\ -s_{10} & 0 & c_{10} \end{bmatrix}$$

$$R_0 R_1 R_2 R_3 = R_8 R_5 R_4 \tag{3.12}$$

Table 3.6: Joint positions

Name	Short description of the position
O_0	Rear wheel contact patch
O_1	Lowest point in the rear wheel torus centerline
O_2	Center of the rear wheel hub
O_3	Joint between swingarm and main body
O_4	Steering joint: joint between main body and steering head
O_5	Center of the front wheel hub
O_6	Lowest point in the front wheel torus centerline
O_7	Front wheel contact patch
Om_i	position of mass center of body i

The rotation matrices are stated above. Note that each rotation is a basic rotation. Vectors are used for pointing to a specific joint or location inside the model. A vector can be expressed with respect to a frame as a column of length three. To point to a location inside the model in the global frame, the vector must undergo several rotations. Rotation matrices are used to perform a rotation of a vector. The rotation matrix can be seen as a new set of unit length vectors, perpendicular to each other, that together form a new reference frame. With rotation matrices, a vector can simply be rotated by pre-multiplying the column with the rotation matrix. Another way to look at this is to observe that the vector is expressed w.r.t. the rotation matrix (which, as already explained, is just another frame). Of course, three unit length vectors can be expressed w.r.t. any frame, not only the inertial reference frame. Therefore, the three unit length vectors of a frame can be expressed w.r.t another frame. Frames with multiple rotations can therefore be build from several basic rotations. The basic frames may have no physical meaning when considered separately. They only mean something in combination with other frames. In short, a position is described by a vector which is represented by a column of length three. The matrix that is in front of the vector is the frame in which the vector is expressed. Note that the derived coordinates follow from the equality in (3.12). Both frames (the left and right expression in (3.12)) in this expression are orientated such that the z-axis is in the same direction as the motorcycle steering axis. The x-axis is in longitudinal direction of the front part of the motorcycle, and the y-axis is oriented in the lateral direction of the front part of the motorcycle.

The position vectors pointing to the center of mass of a body, and the origin of a force or torque are expressed in this section. In the first case, that specific point is denoted with Om_i. In the latter, that point will be a rotation point, and is denoted with O_i. There are eight rotation points in the model. The eight rotation points are summarized in table 3.6, and the expressions are given in (3.13). Note that the expression for R_4 and R_5 is quite large since q_4 and q_5 are dependent coordinates. Therefore, the expression for the front wheel contact patch has been rewritten so that the evaluation of this vector expression is in a simpler form.

$$\begin{aligned}
O_0 &= O_4 + R_0\left(R_1\left(R_2\mathbf{d_1} + R_6\mathbf{d_4} + \mathbf{b_r}\right)\right) + \mathbf{c_r} \\
O_1 &= O_4 + R_0\left(R_1\left(R_2\mathbf{d_1} + R_6\mathbf{d_4} + \mathbf{b_r}\right)\right) \\
O_2 &= O_4 + R_0\left(R_1\left(R_2\mathbf{d_1} + R_6\mathbf{d_4}\right)\right) \\
O_3 &= O_4 + R_0\left(R_1\left(R_2\mathbf{d_1}\right)\right) \\
O_4 &= \begin{bmatrix} x_0 & y_0 & z_0 \end{bmatrix}^T \\
O_5 &= O_4 + R_0\left(R_1\left(R_2\left(R_3\mathbf{d_2}\right)\right)\right) \\
O_6 &= O_4 + R_0\left(R_1\left(R_2\left(R_3\left(\mathbf{d_2} + R_4\mathbf{b_f}\right)\right)\right)\right) \\
O_7 &= O_4 + R_0\left(R_1\left(R_2\left(R_3\left(\mathbf{d_2} + R_4\left(\mathbf{b_f} + R_5\mathbf{c_f}\right)\right)\right)\right)\right) \\
&= O_4 + R_0\left(R_1\left(R_2\left(R_3\mathbf{d_2}\right)\right)\right) + R_8\left(R_5^T\mathbf{b_f}\right) + \mathbf{c_f}
\end{aligned} \tag{3.13}$$

where

$$\begin{array}{ll}
\mathbf{c_r} = [& 0 \quad 0 \quad -c_r \quad]^T \\
\mathbf{b_r} = [& 0 \quad 0 \quad -b_r \quad]^T \\
\mathbf{d_4} = [& -d_4 \quad 0 \quad 0 \quad]^T \\
\mathbf{d_1} = [& -d_1 \quad 0 \quad 0 \quad]^T \\
\mathbf{d_2} = [& d_3 \quad 0 \quad -d_2 \quad]^T \\
\mathbf{b_f} = [& 0 \quad 0 \quad -b_f \quad]^T \\
\mathbf{c_f} = [& 0 \quad 0 \quad -c_f \quad]^T
\end{array} \tag{3.14}$$

The expressions for the center of mass positions are stated as

$$\begin{array}{ll}
Om_1 = & O_2 \\
Om_2 = & O_4 + R_0\left(R_1\left(R_2\mathbf{d_1} + R_6\mathbf{p_2}\right)\right) \\
Om_3 = & O_4 + R_0\left(R_1\left(R_2\mathbf{p_3}\right)\right) \\
Om_4 = & O_4 + R_0\left(R_1\left(R_2\left(R_3\mathbf{p_4}\right)\right)\right) \\
Om_5 = & O_4 + R_0\left(R_1\left(R_2\left(R_3\mathbf{d_2} + \mathbf{p_5}\right)\right)\right) \\
Om_6 = & O_5
\end{array} \tag{3.15}$$

where

$$\begin{array}{ll}
\mathbf{p_2} = [& p_{2x} \quad 0 \quad p_{2z} \quad]^T \\
\mathbf{p_3} = [& p_{3x} \quad 0 \quad p_{3z} \quad]^T \\
\mathbf{p_4} = [& p_{4x} \quad 0 \quad p_{4z} \quad]^T \\
\mathbf{p_5} = [& p_{5x} \quad 0 \quad p_{5z} \quad]^T
\end{array} \tag{3.16}$$

$$\begin{array}{ll}
Rm_1 = & R_0R_1R_9 \\
Rm_2 = & R_0R_1R_6R_{p2} \\
Rm_3 = & R_0R_1R_2R_{p3} \\
Rm_4 = & R_0R_1R_2R_3R_{p4} \\
Rm_5 = & R_0R_1R_2R_9R_{p5} \\
Rm_6 = & R_0R_1R_2R_3R_{10}
\end{array} \tag{3.17}$$

The orientation of the mass center can be calculated with (3.17). For a body to be able to have any orientation in three dimensional space, it should have three rotations. The orientation of body 4, 5 and 6 are expressed with more than three rotations. Extra rotations mean that the equations of motion will get more complicated, which is not desired. The second model, developed at the end of this chapter, will not have these extra terms. Note from (3.17), that each body undergoes one rotation that is fixed. this fixed rotation is there to be able to have the axes from the frame coincide with the principal axes of the body.If this rotation is zero, then the frame of the body will have a orientation similar to the nearest joint.

$$\begin{array}{ll}
R_{p2} = \begin{bmatrix} \cos(p_{2q}) & 0 & \sin(p_{2q}) \\ 0 & 1 & 0 \\ -\sin(p_{2q}) & 0 & \cos(p_{2q}) \end{bmatrix} & R_{p3} = \begin{bmatrix} \cos(p_{3q}) & 0 & \sin(p_{3q}) \\ 0 & 1 & 0 \\ -\sin(p_{3q}) & 0 & \cos(p_{3q}) \end{bmatrix} \\
R_{p4} = \begin{bmatrix} \cos(p_{4q}) & 0 & \sin(p_{4q}) \\ 0 & 1 & 0 \\ -\sin(p_{4q}) & 0 & \cos(p_{4q}) \end{bmatrix} & R_{p5} = \begin{bmatrix} \cos(p_{5q}) & 0 & \sin(p_{5q}) \\ 0 & 1 & 0 \\ -\sin(p_{5q}) & 0 & \cos(p_{5q}) \end{bmatrix}
\end{array} \tag{3.18}$$

3.4 Forces acting on the motorcycle

The final ingredient before the equations of motion can be derived are the forces and torques. The forces have been mentioned before. It was said that there are seven forces and nine torques, but it is not so convenient to differentiate between forces and torques in the virtual work. It is more convenient to distinguish the virtual work terms in different levels of complexity. The easiest terms are the control inputs, being the engine torque, steering torque, front and rear brake torque. These terms are so simple that (3.6) doesn't have to be used at all. These torques are directly related to a specific degree of freedom. The next level are the virtual suspension work terms. Although front suspension origins from a force, and rear suspension from a torque, they can be categorized at the same level. Next level are the tire forces which are more complax. The separate virtual work terms are summarized in Table 3.7, with their name and description.

Table 3.7: Virtual work terms that are present in the motorcycle model

Symbol	Description
Q_{u1}	virtual work done by steering joint torque
Q_{u2}	virtual work done by engine torque
Q_{u3}	virtual work done by rear wheel brake torque
Q_{u4}	virtual work done by front wheel brake torque
Q_{sr}	virtual work done by rear suspension torque
Q_{sf}	virtual work done by front suspension force
Q_{zr}	virtual work done by vertical component of rear tire force
Q_{zf}	virtual work done by vertical component of front tire force
Q_{tr}	virtual work done by lateral (transversal) component of rear tire force
Q_{tf}	virtual work done by lateral (transversal) component of front tire force
Q_{mr}	virtual work done by moment from lateral component of rear tire force
Q_{mf}	virtual work done by moment from lateral component of front tire force
Q_{lr}	virtual work done by longitudinal component of rear tire force
Q_{lf}	virtual work done by longitudinal component of front tire force
Q_{nr}	virtual work done by moment from longitudinal component of rear tire force
Q_{nf}	virtual work done by moment from longitudinal component of front tire force

control input torques

The four control inputs are steering torque, engine torque, rear brake torque, and front brake torque. These control inputs, together with their symbol, are summarized in table 3.8. The control inputs are the only non-dissipative forces that can put energy in the system. To obtain the contribution of each of these torques to the equations of motion, the calculus of small variations has been used. All generalized coordinates are kept constant, except for one. During variation of this single coordinate, the torque is kept constant. This is done for all coordinates.

The steering torque is applied to the steering joint. It is not hard to see that the only case in which this torque delivers work is when the steering angle (q_3) is varied. The amount of work done is exactly the torque applied, and therefore, this applied force term can be stated as

$$Q_{u1} = \begin{bmatrix} 0 & 0 & 0 & 0 & 0 & 0 & u_1 & 0 & 0 & 0 & 0 \end{bmatrix}^T \tag{3.19}$$

Table 3.8: control input torques applied to the motorcycle

Symbol	Description
u_1	Steering joint torque
u_2	Engine torque
u_3	Rear wheel brake torque
u_4	Front wheel brake torque

The engine torque will yield work when the rear wheel rotation is varied, and when the main body is rotated around the pitch angle. The work done depends on the specific configuration of the transmission of the work from the engine to the wheel. In this specific model, it is assumed that the work done when varying q_9 is similar, but opposite to, q_2. Then, the virtual work done by this term is as

$$Q_{u2} = \begin{bmatrix} 0 & 0 & 0 & 0 & 0 & -u_2 & 0 & 0 & 0 & u_2 & 0 \end{bmatrix}^T \tag{3.20}$$

$$Q_{u3} = \begin{bmatrix} 0 & 0 & 0 & 0 & 0 & 0 & 0 & -u_3 sign(\dot{q}_6) & 0 & u_3 sign(\dot{q}_9) & 0 \end{bmatrix}^T \tag{3.21}$$

The brake torque will also yield work when the rear wheel rotation is varied. The brake caliper is mounted to the swingarm. Therefore, in contrary to the engine torque, the brake torque will not supply work when q_2 is varied, but when q_6 is varied. A brake can only dissipate energy from system. The brake torque can therefore only be opposite to the velocity. To take that into account, the terms in (3.21) have a multiplication by the sign of the angular velocity.

suspension virtual work

$$\begin{aligned} F_{sr} &= k_2(q_2 - q_6 - q_{70}) + b_2(\dot{q}_2 - \dot{q}_6) \\ F_{sf} &= k_3(d_2 - d_{20}) + b_3\dot{d}_2 \end{aligned} \tag{3.22}$$

Next level in complexity is the virtual work done by the suspension. The suspension force includes some constants and velocities. The constants are summarized in table 3.9. The force and torque are given in (3.22). The virtual work done by these forces can again be obtained relatively easy with the calculus of variations, so there is no need to use (3.6). The virtual work term is given as

$$\begin{aligned} Q_{sr} &= \begin{bmatrix} 0 & 0 & 0 & 0 & 0 & -F_{sr} & 0 & F_{sr} & 0 & 0 & 0 \end{bmatrix}^T \\ Q_{sf} &= \begin{bmatrix} 0 & 0 & 0 & 0 & 0 & 0 & 0 & 0 & -F_{sf} & 0 & 0 \end{bmatrix}^T \end{aligned} \tag{3.23}$$

tyre virtual work

The tire force is the most complex force in the system. The tire force is a force that is acting in the contact patch of each wheel. Actually, the tire contact patch is a surface with a certain pressure

Table 3.9: force parameters used for the suspension

Constant	Description
k_2	Rear suspension spring stiffness
k_3	Front suspension spring stiffness
b_2	Rear suspension damping constant
b_3	Front suspension damping constant
q_{70}	Rear suspension spring neutral angle
d_{20}	Front suspension spring neutral length

and shear distribution. The pressure distribution can be replaced by a net force perpendicular to the surface. The shear stress can be replaced by a force parallel to the surface. The force representing the shear stress can be decomposed into a force longitudinal to the wheel, and a force lateral to the wheel.

The target of the net perpendicular force must lie within the surface area. The net force can be translated to any other point in the rigid body, in this case the wheel. When translating the force, an extra moment arises and has to be taken into account. It is assumed that there is no moment when the force is in the point O_0 for the rear wheel, and O_7 for the front wheel. This assumption is of course a simplification of reality. It is probably more accurate to assume that the net force having zero moment is slightly in front of O_0 and O_7, because only then, rolling resistance can be included. The latter assumption is left open for further research. It is believed that the increased accuracy in modeling does not outweigh the inaccuracy in the extra parameters that have to be estimated.

The net force perpendicular to the contact patch surface area is the 'tire vertical force', F_{zr} for the rear wheel, and F_{zf} for the front wheel. The equations for these forces is quite involved. The vertical force will be important for calculating the shear forces as well, and thus, has to be accurate. The expression for this force evolves from a simple linear spring. Simulation of the model revealed that the tire kept on bouncing, so a damper was added. Then, negative forces were observed. Since a road cannot pull on a tire, the negative forces were eliminated by summing the force with its absolute, and dividing by 2. These steps are visualized in table 3.10. Note that a simple abs could have been used in the third step, instead of the $\sqrt{F_z^2}$, but is not done because an abs cannot be differentiated symbolically, which is needed for the model to be linearized. The last step in the evolution of the vertical force is necessary to get rid of positive forces when the wheel is not touching the ground. This occurred after so called wheelies, when the vertical velocity is highly negative, and the vertical position is barely positive. In the last term, a relaxation constant has been introduced to avoid division by zero. The relaxation constant was a numerical necessity, but accidentally increased the accuracy with the expected behavior.

tire vertical force

$$z_r = O_0 \cdot [\overset{\circ}{\underset{\mathrm{I}}{\circ}}] \tag{3.24}$$

$$z_f = O_7 \cdot [\overset{\circ}{\underset{\mathrm{I}}{\circ}}] \tag{3.25}$$

$$\dot{z}_r = \frac{dz_r}{dt} = \frac{\partial z_r}{\partial q}\frac{\partial q}{\partial t} = \sum_{i=1}^{11} \frac{\partial z_r}{\partial q_i}\dot{q}_i \tag{3.26}$$

Table 3.10: evolution of the tire vertical force

step	Tire vertical force
1	$F_z = -k \cdot z$
2	$F_z = -k \cdot z - b \cdot \dot{z}$
3	$F_z = \frac{1}{2}((-k \cdot z - b \cdot \dot{z}) + \sqrt{(-k \cdot z - b \cdot \dot{z})^2})$
4	$F_z = \frac{1}{4}((-k \cdot z - b \cdot \dot{z}) + \sqrt{(-k \cdot z - b \cdot \dot{z})^2}) \frac{(z-\sqrt{z^2})z}{(z^2+d/k)}$

Table 3.11: force parameters used for the tire vertical force

Constant	Description
k_1	Rear tire vertical spring stiffness
k_4	Front tire vertical spring stiffness
b_1	Rear tire vertical damping constant
b_4	Front tire vertical damping constant
d_r	Rear tire relaxation parameter
d_f	Front tire relaxation parameter

$$\dot{z}_f = \frac{dz_f}{dt} = \frac{\partial z_f}{\partial q}\frac{\partial q}{\partial t} = \sum_{i=1}^{11} \frac{\partial z_f}{\partial q_i}\dot{q}_i \tag{3.27}$$

$$F_{zr} = \frac{1}{4}((-k_1 z_r - b_1 \dot{z}_r) + \sqrt{(-k_1 z_r - b_1 \dot{z}_r)^2}) \frac{(z_r - \sqrt{z_r^2})z_r}{(z_r^2 + d_r/k_1)} \tag{3.28}$$

$$F_{zf} = \frac{1}{4}((-k_4 z_f - b_4 \dot{z}_f) + \sqrt{(-k_4 z_f - b_4 \dot{z}_f)^2}) \frac{(z_f - \sqrt{z_f^2})z_f}{(z_f^2 + d_f/k_4)} \tag{3.29}$$

The calculation of the tire vertical force requires information about the vertical position and velocity of the tire contact patch. The vertical position can be calculated with (3.24) for the rear wheel, and (3.25) for the front wheel. The vertical velocities can be calculated with (3.26) for the rear wheel, and (3.27) for the front wheel. Furthermore, the expression of the vertical tire force contains a number of parameters. These parameters are listed in Table 3.9

virtual work done by the tire vertical force

The work done by the vertical tire forces is too complex to write down purely by insight. Therefore, Equation 3.6 has to be used. For the vertical force, the equation is written as

$$Q_{zr} = \frac{\partial O_i}{\partial q}^T \cdot F_i = \frac{\partial O_0}{\partial q}^T \begin{bmatrix} 0 & 0 & F_{zr} \end{bmatrix}^T \tag{3.30}$$

Table 3.12: Contact patch velocities and their names

Name	Description
v_{zr}	Rear contact patch vertical velocity
v_{tr}	Rear contact patch transversal (lateral) velocity
v_{lr}	Rear contact patch longitudinal velocity
v_{zf}	Front contact patch vertical velocity
v_{tf}	Front contact patch transversal (lateral) velocity
v_{lf}	Front contact patch longitudinal velocity

$$Q_{zf} = \frac{\partial O_i}{\partial q}^T \cdot F_i = \frac{\partial O_7}{\partial q}^T \begin{bmatrix} 0 & 0 & F_{zf} \end{bmatrix}^T \tag{3.31}$$

tire lateral force

This section explains the derivation of the tire lateral force. The derivation of the tire lateral force is not straightforward and there are some snags in it. First, the force itself is derived from the linear tire model used in [16]. The force is stated in Equation 3.35. b_{tr} is the rear wheel lateral slip stiffness or cornering stiffness. F_{zr} is the rear tire vertical force as has been explained in the previous section. The rest of this tem is called the slip angle in [16]. The only difference with [16] is that this term contains the relaxation parameter d_{tr}. The relaxation parameter d_{tr} was added to make the expression differentiable when the forward velocity is zero. The contact patch lateral and longitudinal velocities are summarized in table 3.12, and can be calculated in a similar manner as the tire vertical velocity in the previous section. The expression for the contact patch lateral and longitudinal velocities are stated in equation 3.34. Note that the velocities for the front wheel contact patch become quite elaborate since they are dependent of almost all coordinates. Equation 3.32 shows that the lateral and longitudinal velocities are calculated in cartesian coordinates. Calculating the tangential position first, and then differentiating is also possible, and leads to a similar expression. When calculating the tangential position first, polar coordinates are used, and the chain rule has to be applied.

$$\begin{aligned} v_{tr} &= -\sin(q_0)v_{xr} + \cos(q_0)v_{yr} \\ v_{lr} &= \cos(q_0)v_{xr} + \sin(q_0)v_{yr} \\ v_{tf} &= -\sin(q_8)v_{xf} + \cos(q_8)v_{yf} \\ v_{lf} &= \cos(q_8)v_{xf} + \sin(q_8)v_{yf} \end{aligned} \tag{3.32}$$

$$\begin{aligned} x_r &= O_0 \cdot \begin{bmatrix} 1 \\ 0 \\ 0 \end{bmatrix} & x_f &= O_7 \cdot \begin{bmatrix} 1 \\ 0 \\ 0 \end{bmatrix} \\ y_r &= O_0 \cdot \begin{bmatrix} 0 \\ 1 \\ 0 \end{bmatrix} & y_f &= O_7 \cdot \begin{bmatrix} 0 \\ 1 \\ 0 \end{bmatrix} \end{aligned} \tag{3.33}$$

$$\begin{aligned} v_{xr} &= \frac{dx_r}{dt} = \sum_{i=1}^{11} \frac{\partial x_r}{\partial q_i}\dot{q}_i & v_{xf} &= \frac{dx_f}{dt} = \sum_{i=1}^{11} \frac{\partial x_f}{\partial q_i}\dot{q}_i \\ v_{yr} &= \frac{dy_r}{dt} = \sum_{i=1}^{11} \frac{\partial y_r}{\partial q_i}\dot{q}_i & v_{yf} &= \frac{dy_f}{dt} = \sum_{i=1}^{11} \frac{\partial y_f}{\partial q_i}\dot{q}_i \end{aligned} \tag{3.34}$$

$$F_{tr} = b_{tr} \cdot F_{zr} \cdot \arctan\left(\frac{-v_{tr} \cdot v_{lr}}{v_{lr}^2 + d_{tr}}\right), \qquad F_{tf} = b_{tf} \cdot F_{zf} \cdot \arctan\left(\frac{-v_{tf} \cdot v_{lf}}{v_{lf}^2 + d_{tf}}\right) \tag{3.35}$$

virtual work done by the tire lateral force

When calculating the virtual work done by the lateral force, a snag pops up. If the virtual work is calculated with (3.6), something peculiar is happening. To see this, the position vector of the rear wheel, together with (3.6) are restated in (3.36). Something similar is happening for the front tire, but for convenience it is only explained for the rear wheel.

$$\begin{aligned} &W\left(q, \dot{q}\right) = \textstyle\sum_{i=1}^{7} \frac{\partial O_i}{\partial q}^T \cdot F_i \\ &O_0 = O_4 + R_0\left(R_1\left(R_2\mathbf{d_1} + R_6\mathbf{d_4} + \mathbf{b_r}\right)\right) + \mathbf{c_r} \end{aligned} \tag{3.36}$$

When O_0 is substituted in W, it will be differentiated with respect to the generalized coordinates. Since $\mathbf{c_r}$ is not a function of the generalized coordinates, it's time derivative disappears. The information will be lost. At first instance, this is against intuition, since the position where the force is acting is very important. $\frac{\partial O_0}{\partial q}$ will become identical to $\frac{\partial O_1}{\partial q}$, while these positions are clearly distinct. Something similar will happen to the longitudinal force in the next section, but then it is not only $\mathbf{c_r}$ that disappears, but also $\mathbf{b_r}$. So the force that is acting in the contact patch delivers work as if it is in the wheel centre.

To see the origin of this problem, the calculus of variations is applied and inspected. It becomes clear that the force is delivering work in one direction, but displaces over the tire in the in the opposite direction. These phenomena cancel each other.

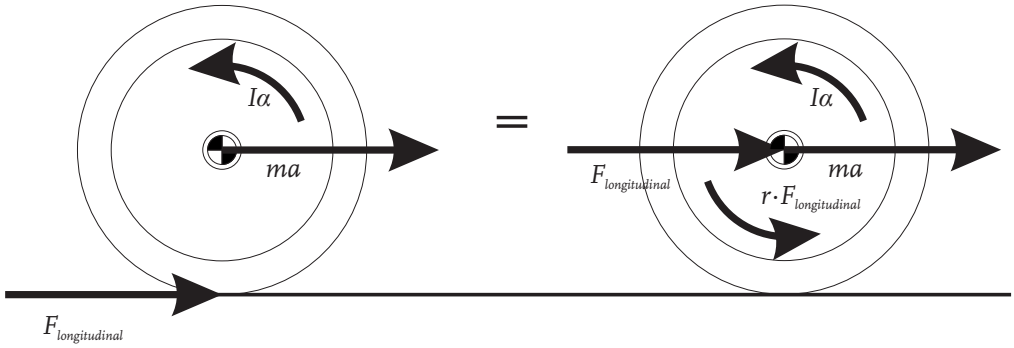

Figure 3.8: translation of longitudinal force from contact patch to hub.

Because this error is not tolerable, another solution has been applied. The principle of d'Alembert states that a dynamic system can be turned into a static system by applying a force that will counteract the acceleration. Applying this theorem several times means that one can translate the force as long as the force stays within the rigid body, and an appropriate moment is added. This is also explained in Figure 3.8. There, the longitudinal force in the contact patch is replaced by a force and a moment in the center of the wheel.

When translating the force, a moment with a magnitude that is the force times the displacement pops up. The direction of the moment is perpendicular to the force and the displacement. To minimize the complexity, the force is translated with the minimum distance necessary. This means that the rear

transversal force is translated from O_0 to O_1 and the front transversal force is translated from O_7 to O_6. The virtual work done by this force can now be calculated to be as

$$\begin{aligned} Q_{tr} &= \tfrac{\partial O_1}{\partial q}^T \cdot \begin{bmatrix} -s_0 F_{tr} & c_0 F_{tr} & 0 \end{bmatrix}^T \\ Q_{tf} &= \tfrac{\partial O_6}{\partial q}^T \cdot \begin{bmatrix} -s_8 F_{tf} & c_8 F_{tf} & 0 \end{bmatrix}^T \end{aligned} \tag{3.37}$$

The virtual work done by the moment that arises can be deduced by insight for the rear wheel and is given in (3.38).The virtual work done by the moment from the front wheel lateral force can be deduced with the calculus of variations. The moment of the rear wheel is in the q_1 direction. Similar, the moment of the front wheel is in the q_5 direction. However, q_5 is not a generalized direction, but a derived direction. Therefore, the contribution of this moment to the applied force term cannot be simply plugged in a certain coordinate. The contribution of this moment is distributed over the q_1, q_2 and q_3 direction. the distribution is given by the derivative of q_5 w.r.t. the generalized coordinates. It helps to think what work the moment would do when varying q_1, q_2 and q_3 respectively. The expression for the moment from the front wheel lateral moment is given as

$$Q_{mr} = \begin{bmatrix} 0 & 0 & 0 & 0 & F_{tr} \cdot c_r & 0 & 0 & 0 & 0 & 0 & 0 \end{bmatrix}^T \tag{3.38}$$

$$Q_{mf} = -\frac{dq_5}{dq}^T \cdot c_f \cdot F_{tf} \tag{3.39}$$

tire longitudinal force

The tire longitudinal force is also calculated from the equation in [16]. The velocities in this expression can be calculated with (3.32).The expression for the tire longitudinal force is given in (3.40). b_{lr} and b_{lf} are the longitudinal tire stiffness. The last part of this term is the difference in velocity between the road and the tire contact patch.

$$F_{lr} = b_{lr} \cdot F_{zr} \cdot \left(\left(b_r + c_r \cos(q_1) \right) q_{9d} - v_{lr} \right), \qquad F_{lf} = b_{lf} \cdot F_{zf} \cdot \left(\left(b_f + c_f \cos(-q_5) \right) q_{10d} - v_{lf} \right) \tag{3.40}$$

virtual work done by the tire longitudinal force

A problem similar to the one that occurred when calculating the virtual work done by the lateral forces occurs when calculating the virtual work done by the longitudinal forces. This time, the problem can only be solved when the force is translated to the hub of the tire. The work done by the force can easily be calculated with (3.41), but the virtual work done by the moment that arises when displacing the force, is much more elaborate. The virtual work from the moment coming from the rear wheel longitudinal force is given in (3.43). In (3.43), $(O_5 - O_7)$ is the displacement of the force, or in other words, the arm. $R_8 \cdot \begin{bmatrix} 0 & 0 & 0 \end{bmatrix}^T$ is the direction of the force. By taking the external product with the generalized coordinate, the work done by the moment in that direction is calculated. This is because the moment is perpendicular to the force and the displacement.

$$\begin{aligned} Q_{lr} &= \tfrac{\partial O_2}{\partial q}^T \cdot \begin{bmatrix} c_0 F_{tr} & s_0 F_{tr} & 0 \end{bmatrix}^T \\ Q_{lf} &= \tfrac{\partial O_5}{\partial q}^T \cdot \begin{bmatrix} c_8 F_{tf} & s_8 F_{tf} & 0 \end{bmatrix}^T \end{aligned} \tag{3.41}$$

$$Q_{nr} = \begin{bmatrix} 0 & 0 & 0 & -b_r \cdot s_1 \cdot F_{lr} & 0 & 0 & 0 & 0 & 0 & (-b_r - c_r \cdot c_1) \cdot F_{lr} & 0 \end{bmatrix}^T \tag{3.42}$$

$$Q_{nf} = \begin{bmatrix} 0 \\ 0 \\ 0 \\ -b_f \cdot \sin(-q_5) \\ \left(R_0 R_1 \left[\begin{smallmatrix} 1 \\ 0 \end{smallmatrix}\right] \times R_8 \left[\begin{smallmatrix} 1 \\ 0 \end{smallmatrix}\right]\right)^T \cdot (O_5 - O_7) \\ \left(R_0 R_1 R_2 \left[\begin{smallmatrix} 0 \\ 0 \end{smallmatrix}\right] \times R_8 \left[\begin{smallmatrix} 1 \\ 0 \end{smallmatrix}\right]\right)^T \cdot (O_5 - O_7) \\ \left(R_0 R_1 R_2 \left[\begin{smallmatrix} 0 \\ 1 \end{smallmatrix}\right] \times R_8 \left[\begin{smallmatrix} 1 \\ 0 \end{smallmatrix}\right]\right)^T \cdot (O_5 - O_7) \\ 0 \\ 0 \\ 0 \\ (-b_f - c_f \cos(-q_5)) \end{bmatrix} \cdot F_{lf} \tag{3.43}$$

3.5 Equations of motion

In the previous sections all the ingredients that are needed to calculate the equations of motion are discussed. Now that the different variables and terms are defined, the equations of motion can be derived. The applied force term is already calculated in the previous section and only need to be summed.

$$Q = Vq^T + Q_{zr} + Q_{sr} + Q_{sf} + Q_{zf} + Q_{tr} + Q_{mr} + Q_{tf} + Q_{mf} + Q_{lr} + Q_{nr} + Q_{lf} + Q_{nf} + Q_{u1} + Q_{u2} + Q_{u3} + Q_{u4} \tag{3.44}$$

The mass matrix and Christoffel matrix can simply be calculated with the formulas given in (3.2) and (3.4). This calculation is a straightforward job, and is not elaborated further in this text. The mass matrix can be found in appendix C. Some notes can be made about the equations of motion.

First, when using the parameters as in previous sections, the complete set of equations uses about 500.000 characters. That is when all subexpressions (such as the velocities), are evaluated and substituted in the equations of motion. Since there are 11 equations, it means that there are around 45.000 characters per equation. The mass matrix is around 18.000 characters, and the Christoffel matrix is around 100.000 characters. The nonconservative force term is around 360.000 characters. Note that the mass matrix was derived by hand, which saved a lot of characters. the symbolically calculated mass matrix contained 200.000 characters. A lot of characters could probably be saved when the Christoffel matrix and nonconservative force terms are also calculated by hand. The Matlab command 'simple' is too simple and is not well suited for equations with a lot of trigonomic functions.

Secondly, The size of the model explodes mainly because of the front wheel lateral and longitudinal forces. These forces (and moments) take up more than half the characters of the total equations of

motion. The character size of these forces could have been 95 percent smaller if q_8 and q_5 were generalized coordinates, instead of dependent coordinates. Also, the orientation of the front wheel, front fork, and steering head is described with more than three rotations. If also q_4 was a generalized coordinate, these mass orientations could have been expressed with only three rotations. The mass matrix woud then be about 20 percent smaller in character size.

To see what is the effect of q_4, q_8 and q_5 being generalized coordinates, another model has been made. That model is the subject appendix D.

3.6 Summary

The equations of motion of a motorcycle model are derived in this chapter. The derivation leads from a description of the parameters and generalized coordinates to a set of position vectors pointing to joints and mass centers in the model. From these vectors, the equations of motion arise by applying Lagrange mechanics. In the derivation process, it was shown that it is important to guard every derivation step since there can arise errors. A convenient guard is a thorough computer visualization of the position vectors, velocity vectors and acceleration vectors.

Chapter 4

Linearization, validation and analysis of the motorcycle model

To get more insight in the motorcycle dynamics, the equations of motion are linearized. This linearization can be performed around any steady state operating point. Many linear motorcycle models exist in literature. Therefore, the linearized equations of motion can be used to compare the model against other models found in literature.

First, in Section 4.1, the equations of motion as derived in chapter three are transformed into a set of 22 first order ordinary differential equations. In Section 4.2, the linearization proces is explained. Then, in section 4.3, parameters from a literature model are inserted and the equations are compared. In section 4.4, another model from literature has been used to validate the model. After the linearized model has been analyzed, the nonlinear model is validated. A nonlinear model created with the simulating software package Matlab/Simulink SimMechanics has been created, with which the model is validated. It turns out that both model show exactly the same behavior up to numerical precision. Finally, the model has been compared with the model from W. Versteden.

4.1 From equations of motion to a set of first order differential equations

The first step in the linearization proces is to rearrange the equations of motion to a set of first order differential equations. The equations of motion as derived in chapter three are given in as.

$$M(q) \cdot \ddot{q} + C(q, \dot{q}) \cdot \dot{q} + P(q) = W(q, \dot{q}) \tag{4.1}$$

From (4.1), it can be seen that the equations of motion are second order. The mathematical toolbox for first order differential equations is more advanced than for second order differential equations. Therefore, it is desirable to have the equations in first order form. This can be done by introducing a new set of variables. The new variables is defined by (4.2). The new set of variables are called the state variables. The state variables describe the state of the system.

$$
\begin{array}{ll}
x_1 \equiv x_0 & y_1 \equiv \dot{x}_0 \\
x_2 \equiv y_0 & y_2 \equiv \dot{y}_0 \\
x_3 \equiv z_0 & y_3 \equiv \dot{z}_0 \\
x_4 \equiv q_0 & y_4 \equiv \dot{q}_0 \\
x_5 \equiv q_1 & y_5 \equiv \dot{q}_1 \\
x_6 \equiv q_2 & y_6 \equiv \dot{q}_2 \\
x_7 \equiv q_3 & y_7 \equiv \dot{q}_3 \\
x_8 \equiv q_6 & y_8 \equiv \dot{q}_6 \\
x_9 \equiv d_2 & y_9 \equiv \dot{d}_2 \\
x_{10} \equiv q_9 & y_{10} \equiv \dot{q}_9 \\
x_{11} \equiv q_{10} & y_{11} \equiv \dot{q}_{10}
\end{array}
\tag{4.2}
$$

With these newly defined variables, (4.1) can be written in the form as (4.3). In (4.3), I is an identity matrix of size eleven. The variables x and y are columns where x_1 to x_{11} and y_1 to y_{11} are stored in respectively.

$$
\begin{bmatrix} I & 0 \\ 0 & M(x) \end{bmatrix} \cdot \begin{bmatrix} \dot{x} \\ \dot{y} \end{bmatrix} = \begin{bmatrix} y \\ W(x,y) - C(x,y) \cdot y - P(x) \end{bmatrix} \tag{4.3}
$$

4.2 Linearization and state space description

Linearization can be made at any steady state point or trajectory. Linearization consists of two steps. The first step is to differentiate the right side of (4.3) w.r.t. the state variables. The result will be a square matrix called the Jacobian matrix. This matrix is dependent of the point around which the linearization will take place, and is clearly time dependent. The next step is to substitute the parameters and generalized coordinates in the state variables at the point around which to linearize. These numbers should be substituted in the Jacobi matrix, as well as in the mass matrix. The linearized set is called a state space description. From this description, it is possible to investigate the stability of the system.

4.3 Validation of the linearized model

The linearized equations of motion can also be used to check the model against other models in literature. To validate the model, a equal set of parameters have to be found as has been used for the model that the current model is compared with. The first comparison is made with Jbike6. The Jbike6 is only a fourth order model, so not only the parameters have to be estimated, also the model has to be simplified.

The Jbike6 has no tire model, it uses a nonholonomic rolling constraint between the wheel and the ground. The nonlinear model is adapted to this simplification by making the tire slip stiffness very high. Furthermore, the Jbike6 is actually a bike model, instead of a motorcycle model. That means that some parameters might seem odd, for example the main body yaw inertia, and the main body mass center height are very unlikely to be realistic motorcycle parameters.

Another simplification is the suspension, which is absent in the Jbike6. To cope with this difference, the suspension has a high stiffness parameter, making the suspension very rigid.

Table 4.1: Parameters from the Jbike6

kinematic parameters					
$c_f = c_r = 0$	$d_f = 0.35$	$d_1 = 0.455$	$d_3 = 76{\cdot}10^{-3}$	$d_4 = 0.455$	$d_r = 0.3$
dynamic parameters					
$m_1 = 2$	$I_{1x} = 0.0603$	$I_{1y} = 0.12$		$p_{2q} = 0$	$p_{3q} = -0.63530$
$m_2 = 0$	$I_{2x} = 0$	$I_{2y} = 0$	$I_{2z} = 0$	$p_{2x} = 0$	$p_{2z} = 0$
$m_3 = 85$	$I_{3x} = 6$	$I_{3y} = 11$	$I_{3z} = 6$	$p_{3x} = -0.39$	$p_{3z} = .475$
$m_4 = 4$	$I_{4x} = .06$	$I_{4y} = 0.06$	$I_{4z} = 6{\cdot}10^{-3}$	$p_{4x} = 0.05$	$p_{4z} = -0.2$
$m_5 = 0$	$I_{5x} = 0$	$I_{5y} = 0$	$I_{5z} = 0$	$p_{5x} = 0$	$p_{5z} = 0$
$m_6 = 3$	$I_{6x} = 0.1405$	$I_{6y} = 0.28$		$p_{4q} = -0.17226$	$p_{5q} = 0$
force parameters					
$k_1 = 1{\cdot}10^8$	$b_1 = 1{\cdot}10^3$	$b_{lr} = 20$	$d_{zr} = 1{\cdot}10^{-3}$	$g = 9.81$	
$k_2 = 1{\cdot}10^7$	$b_2 = 1{\cdot}10^3$	$b_{tr} = 2000$	$d_{zf} = 1{\cdot}10^{-3}$	$d_{20} = 0.265$	
$k_3 = 1{\cdot}10^7$	$b_3 = 1{\cdot}10^3$	$b_{lf} = 20$	$d_{tr} = 1{\cdot}10^{-6}$	$q_{70} = 0$	
$k_4 = 1{\cdot}10^8$	$b_4 = 1{\cdot}10^3$	$b_{tf} = 2000$	$d_{tf} = 1{\cdot}10^{-6}$		

initial state values				
$x_1 = -2.8126{\cdot}10^2$	$x_2 = 5.5810{\cdot}10^2$	$x_3 = 6.5559{\cdot}10^{-1}$	$x_4 = 2.0296{\cdot}10^0$	$x_5 = -8.4942{\cdot}10^{-7}$
$x_6 = -2.9043{\cdot}10^{-1}$	$x_7 = 9.2614{\cdot}10^{-9}$	$x_8 = -2.8678{\cdot}10^{-1}$	$x_9 = 3.8792{\cdot}10^{-1}$	$x_{10} = 1.4561{\cdot}10^0$
$x_{11} = -1.0774{\cdot}10^0$	$y_1 =$ varying	$y_2 = 0$	$y_3 = 0$	$y_4 = 2.0504{\cdot}10^{-7}$
$y_5 = -1.2487{\cdot}10^{-7}$	$y_6 = 1.1348{\cdot}10^{-5}$	$y_7 = 1.5860{\cdot}10^{-10}$	$y_8 = -1.6050{\cdot}10^{-4}$	$y_9 = 4.9167{\cdot}10^{-5}$
$y_{10} = 9.4552{\cdot}10^1$	$y_{11} = 9.9283{\cdot}10^1$			

To compare both models, the nonlinear model has been implemented in the computer. A stationary, straight running, operating point has been found by running the model for a while, while resetting the camber angle to zero every once in a while. This has to be done since a camber angle of zero degrees is unstable for most forward speeds. Once all transients disappear in the model, the state variables are extracted from the system. The vanishing of the transients has been monitored. after a few seconds (depending on the starting configuration), the amplitude of all transients was below 10 nanometers in case of a translational degree of freedom, and 10 nanoradians in case of a rotational degree of freedom. The stationary state variables, together with the parameters used, are summarized in table 4.1.

From Table 4.1. it can be seen that the swingarm and the front fork have no mass, and no rotational inertia. The suspension is very stiff, and the joint that connects the main frame to the swingarm has been taken in between the steering head and the rear wheel hub. Some values for the initial state variables are unimportant. For example, the state variables x_1, x_2, and x_3 denote the current position and heading. These states can be anything without affecting the validation proces.

To validate the linearized model, the eigenvalues of the linearized model have been calculated for different forward speeds. Note that all other state variables can remain unchanged while varying the forward speed, except for the rotational velocity of the wheels. There are 22 eigenvalues, most of these eigenvalues are highly negative. Some of the eigenvalues are exactly zero. These eigenvalues originate from the motorcycle position and heading. The eigenvalues are plotted in Figure 4.1. Comparing the eigenvalues in Figure 4.1 with [15] shows a very good agreement of the results.

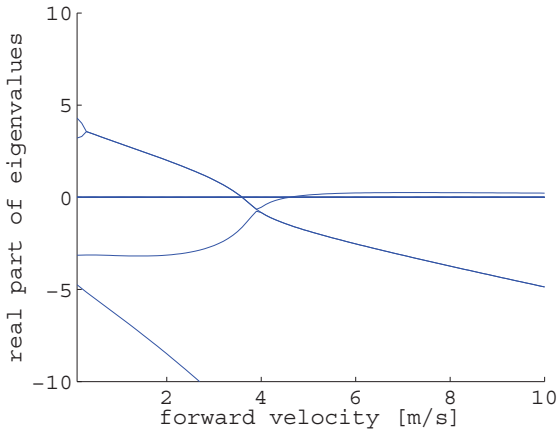

Figure 4.1: Eigenvalues of the linearized model with the Jbike6 parameters inserted [12]

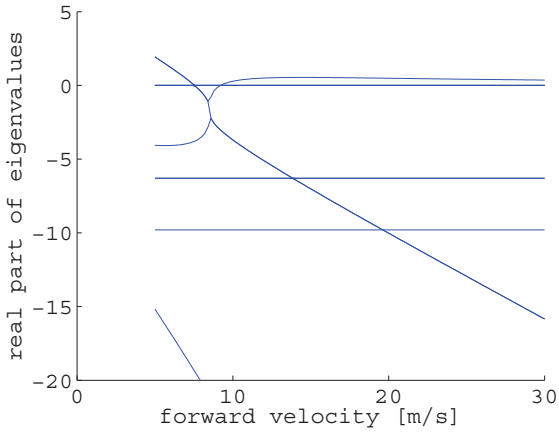

Figure 4.2: Eigenvalues of the linearized model with Koenen parameters inserted

4.4 Validation using the work of Koenen

Another comparison has been made with the model of Koenen; [12], together with the parameters of [26]. The model of Koenen is a motorcycle model, instead of a bike model, so the parameters used in this model are more realistic. The model of Koenen includes a main frame twist axis degree of freedom. This DOF is missing in the model that has been derived in this report. The parameters that are used for the validation are summarized in table 4.2. The eigenvalues are also calculated for this model, and compared with Figure 50 of [12]. Also in this case, both models have similar eigenvalues. There are two minor discrepancies. First, as mentioned before, the twist axis degree of freedom is not present in the new model. Second, the conversion of the parameters of [12] to the parameters used in this model has been an iterative process since there is no straightforward conversion between both parameter sets, resulting in a dynamic model that is slightly different. The difference can be seen in the more negative eigenvalues of the bounce and pitch mode in the model of [12]. It is assumed that this is because of a slightly stiffer suspension on the current model.

Table 4.2: Parameter set of the model of Koenen

kinematic parameters					
$c_f = 0.06$ $c_r = 0.09$	$d_f = 0.319$ $d_r = 0.321$	$d_1 = 0.9214$	$d_3 = 0.066$	$d_4 = 0.4$	
dynamic parameters					
$m_1 = 10$	$I_{1x} = 0.01$	$I_{1y} = 0.34$		$p_{2q} = 0$	$p_{3q} = 0$
$m_2 = 10.6$	$I_{2x} = 0.37$	$I_{2y} = 0$	$I_{2z} = 0.37$	$p_{2x} = -0.3$	$p_{2z} = 0$
$m_3 = 254.1$	$I_{3x} = 15.23$	$I_{3y} = 32$	$I_{3z} = 19.33$	$p_{3x} = -0.5736$	$p_{3z} = 0.044$
$m_4 = 13.1$	$I_{4x} = 0.46$	$I_{4y} = 1.2$	$I_{4z} = 0.21$	$p_{4x} = 0.015$	$p_{4z} = 0.032$
$m_5 = 7.5$	$I_{5x} = 0.29$	$I_{5y} = 0$	$I_{5z} = 0.29$	$p_{5x} = 0.066$	$p_{5z} = 0.632$
$m_6 = 7$	$I_{6x} = 0.01$	$I_{6y} = 0.28$		$p_{4q} = 0$	$p_{5q} = 0$
force parameters					
$k_1 = 1{\cdot}10^6$	$b_1 = 1{\cdot}10^3$	$b_{lr} = 20$	$d_{zr} = 1{\cdot}10^{-3}$	$g = 9.81$	
$k_2 = 1645$	$b_2 = 176$	$b_{tr} = 2000$	$d_{zf} = 1{\cdot}10^{-3}$	$d_{20} = 0.632$	
$k_3 = 9{\cdot}10^3$	$b_3 = 1100$	$b_{lf} = 20$	$d_{tr} = 1{\cdot}10^{-6}$	$q_{70} = -0.9819$	
$k_4 = 1{\cdot}10^6$	$b_4 = 1{\cdot}10^3$	$b_{tf} = 2000$	$d_{tf} = 1{\cdot}10^{-6}$		
initial state values					
$x_1 = 0$	$x_5 = 0$	$x_9 = 0.5980$	$y_1 = \text{var}$	$y_5 = 0$	$y_9 = 0$
$x_2 = 0$	$x_6 = -0.7016$	$x_{10} = 0$	$y_2 = 0$	$y_6 = 0$	$y_{10} = \text{var}$
$x_3 = 0.6888$	$x_7 = 0$	$x_{11} = 0$	$y_3 = 0$	$y_7 = 0$	$y_{11} = \text{var}$
$x_4 = 0$	$x_8 = 0.5415$		$y_4 = 0$	$y_8 = 0$	

4.5 Validation of the nonlinear model using SimMechanics

The ultimate validation of the model is a second multibody model that shows exactly the same dynamic behavior if the same parameters are inserted in both models. To test if a parameter is implemented in the model in the right way, the parameter should not be zero. For the validation, it doesn't care wether the values are realistic or not. Two nonlinear, numerical models have been used for the validation. Random values are substituted in the model parameters and initial conditions. One nonlinear model is obtained from the work done by Versteden ([26]). The nonlinear model made by Versteden uses a completely different tire model. Instead of modeling the tire, the standard car tire block has been adapted to suit large camber angles. For this reason, random parameters were not always possible in this comparison. Another model has been developed in the multibody toolbox of Matlab/Simulink, SimMechanics. This model has been developed completely separate from the model in symbolic form. It uses a similar modeling approach, so that the parameters are identical to the symbolic model derived in chapter three. The dynamic behavior is similar up to eight digits behind the comma for a simulation time of one second. Longer simulation times haven't been done since the computational time of this model is very large.

Figure 4.3 shows the structure of the complete model. The model of the motorcycle is on a lower layer in the block called 'motorcyclemodel'. That block is the most important block. Around this block, there are five other blocks. The name of these blocks should make it clear what is happening inside these blocks. The least important blocks are the derived coordinates calculator block, and the contact patch velocity calculator block. These blocks calculate the dependent coordinates, and the velocity vector of the contact patches. The contact patch velocities can also be obtained directly by measuring inside the motorcyclemodel block. Measuring will give the same values, albeit less accurate. The controller block contains the pilot of the motorcycle, and can only apply a steering torque, and measure the rear camber angle, angular velocity, and the steering angular velocity in this configuration. The controller will be explained in depth in the next chapter. The two blocks in the lower right corner (called "rear wheel forces" and "front wheel forces") calculate the forces acting on the tire contact

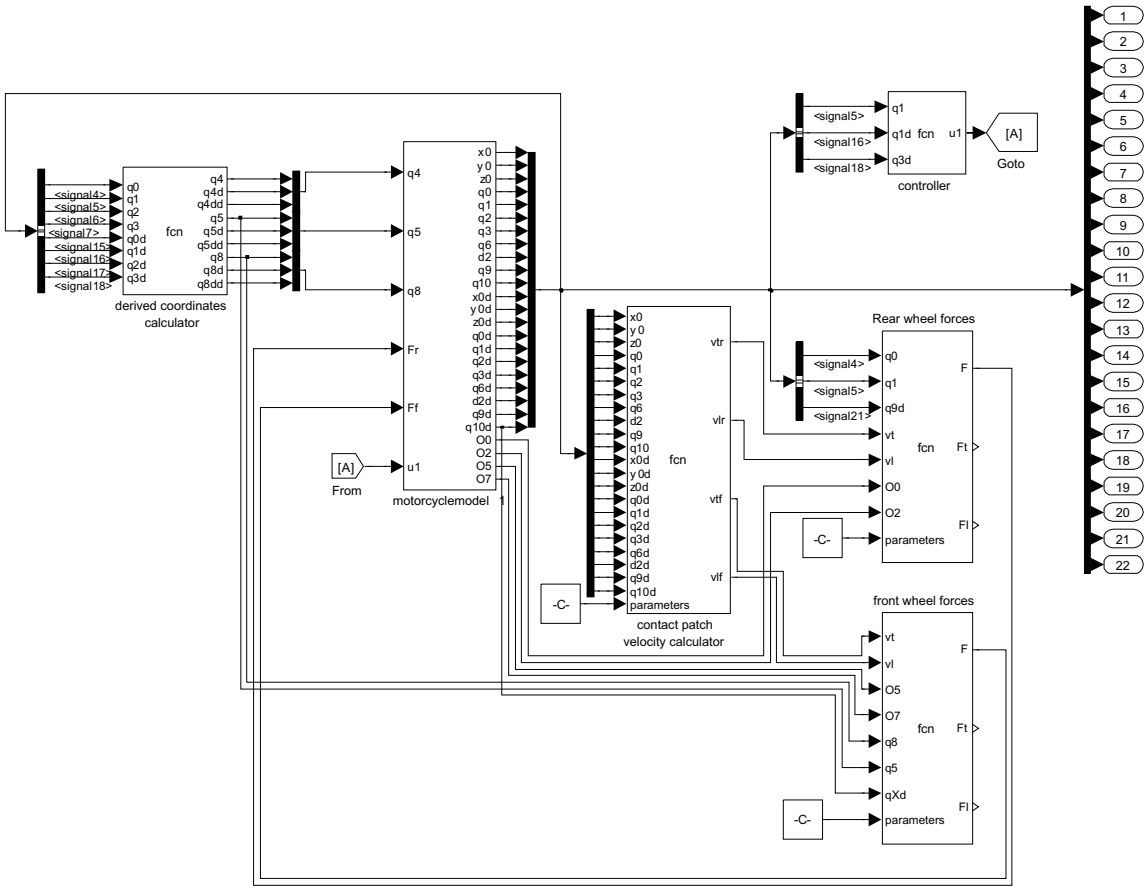

Figure 4.3: Numerical motorcycle model implemented in Matlab/Simulink.

patches. The forces are applied to the wheel center since the virtual work done by the forces when acting in the contact patch cannot be calculated. It is the same problem as has been discussed in previous chapter about the applied forces in the tire contact patch. The tire force blocks outputs a vector of dimension six with the applied moments and applied forces in absolute coordinates.

The inside of the 'motorcyclemodel' block is pictured in figure **??**. This block uses the SimMechanics toolbox of Simulink. An important observation from this figure is that the model looks complicated and cluttered, especially compared with the model created in this report. That model will be shown in the next chapter. What is visible in Figure **??** is that the motorcycle model is a single chain of joints and links, comparable to a robotic manipulator.

For the rest of this report, a different set of parameters are used. The parameters of Koenen are out of date, and specific measurements on the geometry of a Suzuki GSX-R600 have been made. The model with the new set of parameters is more accurate than the set used by Koenen, and the new parameters are categorized also in the book of Cossalter under the category 'performance bikes'. With the new parameters, the wheelbase is 1320 [mm]. The rake is 21 degrees. These numbers are indeed different from the real Suzuki bike, but the exact numbers for the parameters are not that important, as long as the parameters do represent an average 'high performance' motorcycle. The set of parameters is given in Table 4.3.

Table 4.3: high performance bike parameters

kinematic parameters					
$c_f = 0.06$ $c_r = 0.09$	$d_f = 0.3$ $d_r = 0.315$	$d_1 = 0.7$	$d_3 = 0.01$	$d_4 = 0.5$	
dynamic parameters					
$m_1 = 15$	$I_{1x} = 0.3$	$I_{1y} = 0.15$		$p_{2q} = 0$	$p_{3q} = 0$
$m_2 = 10$	$I_{2x} = 0.1$	$I_{2y} = 0.1$	$I_{2z} = 0.1$	$p_{2x} = -0.2$	$p_{2z} = 0$
$m_3 = 220$	$I_{3x} = 6$	$I_{3y} = 6$	$I_{3z} = 6$	$p_{3x} = -0.4$	$p_{3z} = -0.2$
$m_4 = 10$	$I_{4x} = 0.1$	$I_{4y} = 0.1$	$I_{4z} = 0.1$	$p_{4x} = 0.05$	$p_{4z} = -0.2$
$m_5 = 6$	$I_{5x} = 0.1$	$I_{5y} = 0.1$	$I_{5z} = 0.1$	$p_{5x} = -0.05$	$p_{5z} = 0$
$m_6 = 10$	$I_{6x} = 0.2$	$I_{6y} = 0.1$		$p_{4q} = 0$	$p_{5q} = 0$
force parameters					
$k_1 = 1{\cdot}10^6$	$b_1 = 1{\cdot}10^3$	$b_{lr} = 20$	$d_{zr} = 1{\cdot}10^{-3}$	$g = 9.81$	
$k_2 = 15000$	$b_2 = 1500$	$b_{tr} = 2000$	$d_{zf} = 1{\cdot}10^{-3}$	$d_{20} = 0.5$	
$k_3 = 15000$	$b_3 = 1500$	$b_{lf} = 20$	$d_{tr} = 1{\cdot}10^{-6}$	$q_{70} = -0.15$	
$k_4 = 1{\cdot}10^6$	$b_4 = 1{\cdot}10^3$	$b_{tf} = 2000$	$d_{tf} = 1{\cdot}10^{-6}$		
initial state values					
$x_1 = 0$	$x_5 = 0$	$x_9 = 0.406$	$y_1 = \text{var}$	$y_5 = 0$	$y_9 = 0$
$x_2 = 0$	$x_6 = -0.3776$	$x_{10} = 0$	$y_2 = 0$	$y_6 = 0$	$y_{10} = \text{var}$
$x_3 = 0.672$	$x_7 = 0$	$x_{11} = 0$	$y_3 = 0$	$y_7 = 0$	$y_{11} = \text{var}$
$x_4 = 0$	$x_8 = -0.201$		$y_4 = 0$	$y_8 = 0$	

4.6 Stability Analysis of the validated model

In this section, the stability of the system is investigated. A mechanical system is said to be in equilibrium when the net force acting on the body as a whole is zero. This means that the body can be in constant forward motion, or in constant circular motion or at rest. Since the riderless motorcycle is unstable in most riding circumstances, a controller has been developed to stabilize the motorcycle. This means that the motorcycle and controller stay in a stationary point. A feedback torque is applied to the steer that is given in (4.4). In this equation, ref_1 is the reference camber angle. A ref_1 of zero thus means running straight up.

$$u_1 = -1000\,(q_1 - ref_1) - 100\dot{q}_1 \tag{4.4}$$

With the controller in (4.4) added, the system is still not stable. The forward velocity slowly decreases. A second controller has been added to feed back the motorcycle velocity to the engine torque. This controller is given in (4.5). In this equation, ref_2 is the referenced forward velocity.

$$u_2 = -1000\left(\sqrt{\dot{x}_0^2 + \dot{y}_0^2} - ref_2\right) \tag{4.5}$$

Once that a steady state operating point has been found, the model can be linearized around this point, and the eigenvalues can be plotted. The linearization has been made without the controllers, with only the steering controller, and with both controllers applied. In the latter case, all eigenvalues should be negative. Note that the linearization could have been made only once, with both controllers included, because the gains of the controllers can be set to zero, representing the uncontrolled motorcycle. The symbolic linearization proces is very time consuming, but once the parameterized and

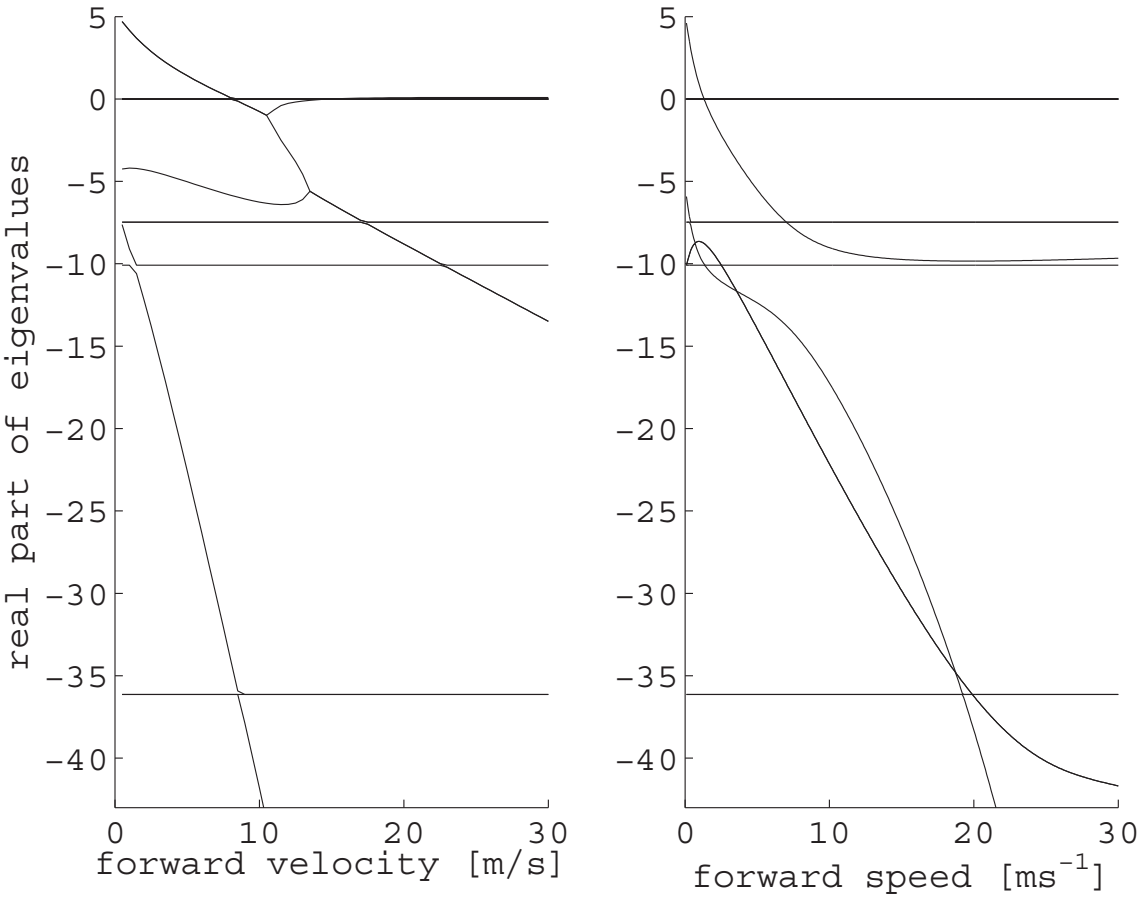

Figure 4.4: velocitysweep without, and with the controller.

linearized equations are obtained, any steady state operating point can be substituted, and the calculation is performed within a hundredth of a second.

Steady state operating points have been found in this way for straight up running at different forward speeds, and for different camber angles at a constant forward velocity of 20 meter per second. In the next section, the eigenvalues for straight up running at different forward speeds are investigated. After that, the eigenvalues for different camber angles at a constant forward velocity of 20 meter per second is investigated.

Eigenvalues for different forward speeds

The eigenvalues of the linearized bike with the parameters listed in table 4.3 are visualized for varying forward velocity in figure 4.4. The diagram in the upper left corner of Figure 4.4 shows the eigenvalues as a function of forward speed for the uncontrolled motorcycle. The solid lines are the real parts of the eigenvalues, and the dashed lines are the imaginary parts of the eigenvalues. Only the eigenvalues between -20 and 20 are shown. There are also some highly negative eigenvalues not shown in the plot of Figure 4.4. These negative eigenvalues probably belong to the tire dynamics, since tire stiffness parameters are around an order in magnitude larger. It can be seen from this figure, that the uncontrolled linearized motorcycle model has positive eigenvalues for almost all forward velocities. In the range from 8.4 m/s to 15 m/s, all eigenvalues are negative. This means that the motorcycle

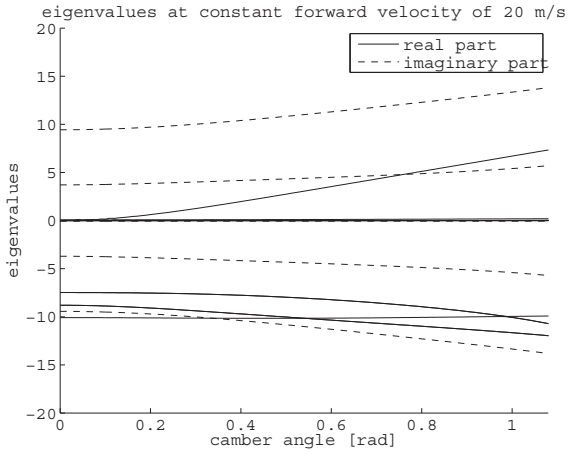

Figure 4.5: Eigenvalues at constant forward speed, and varying camber angle.

should be stable in that operating area. Indeed, a simulation in the time domain shows that the motorcycle is stable for this speed range. Furthermore, the lower left diagram of Figure 4.4 shows that the controlled bike is stable for all forward velocities more than 1.2 meter per second. The motorcycle dynamics completely change upon applying a simple controller. The two solid horizontal lines in the left diagrams are the pitch and bounce mode, while the solid line in the lower left corner is the shake mode. The curved line is a combination of weave and capsize. The pitch and bounce mode are not affected by the controller. The shake and weave mode on the other hand, are changed dramatically. The eigenvalues for different camber angles at a constant speed of 20 meters per second are investigated in next section.

Eigenvalues for different camber angles at 20 meter per second

Steady state operating points also have been found for different camber angles at a constant forward velocity of 20 meter per second. The eigenvalues of the linearized model in these operating points were calculated. Figure 4.5 shows the real part of the eigenvalues as a function of the camber angle for the uncontrolled motorcycle. This figure shows that the pitch and bounce frequency decrease as the camber angle increases. One eigenvalue is becoming increasingly more positive. This positive eigenvalue belongs to the capsizing mode. Figure 4.6 shows the eigenvalues in the complex plane. The figure is subdivided into six figures, where the figure has been zoomed in on different areas. This figure shows the modes that are called shake and weave by Koenen.

The figures will dramatically change when the controller is added. However, the exact shape of the figures of the controlled motorcycle is dependent of the gains chosen. Therefore, it is not meaningful to plot the figures of the controlled motorcycle. A proportional gain of more than 200 is sufficient to stabilize the motorcycle at this speed, at any camber angle from zero to seventy degrees. The differential gain should be more than 10 in order to have the imaginary part of the eigenvalues large enough to suppress oscillations.

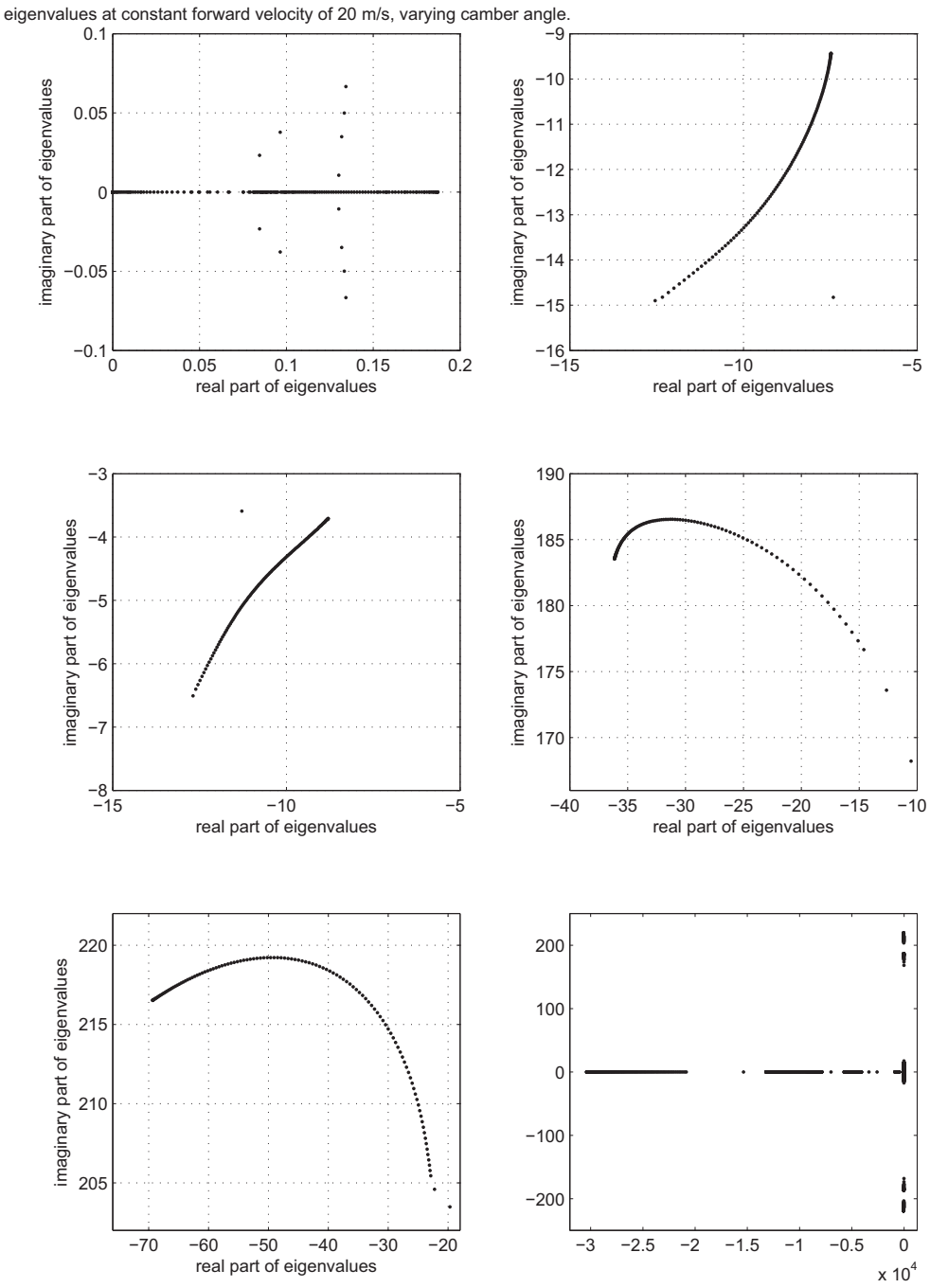

Figure 4.6: Eigenvalues in the complex plane for different camber angles.

Chapter 5

Motorcycle trajectory Control

With a good model at hand, a control strategy can be developed. The model together with the controller are implemented in Matlab/Simulink. A picture of this controller can be seen in Figure 5.1. This picture shows that this model is much neater than the model that has been used for validation. The model in Figure 5.1 has no subsystems or whatsoever. Although the model and the controller blocks in Figure 5.1 have the same size, The model consists of around 700 lines of code, whereas the controller contains only 30. The two integrators at the right side of Figure 5.1 are part of the motorcycle model, and output the generalized velocities and positions respectively. In section 5.1, a discussion of the different control strategies is elaborated in this chapter. In the previous chapter, some simple controllers have already been used. Because the graduation project time is not enough to experiment with all sorts of different exotic controllers, the elaboration is kept to a discussion only. Instead, a controller used in the previous chapter is used to track a signal that represents a circuit course. A combination of feed forward and feedback control is used to keep the motorcycle stable and within the circuit boundaries. This is discussed in Section 5.4. Before that, in Section 5.3, the reference trajectory that should be followed as close as possible by the motorcycle is explained.

5.1 Discussion of different control strategies

The torque applied to the steering head should be such that the motorcycle model will be stable, and that it will track a certain reference trajectory in the ground plane. The first priority is being stable, the second is to follow the trajectory on the road. Following a line in the ground plane can be done in several ways. Three promising categories of control are learning controllers, model predictive controllers, and camber tracking control, which is a proportional feedback gain with reference path

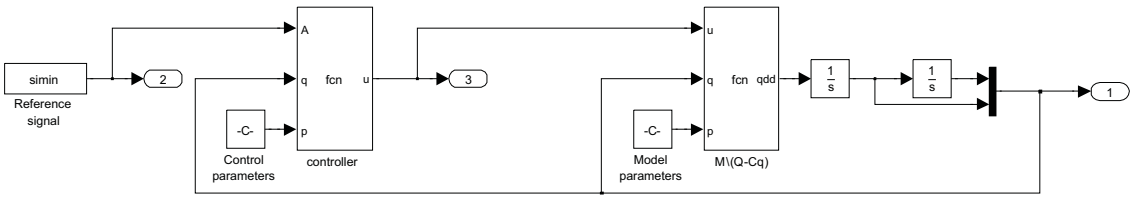

Figure 5.1: controller embedded in Matlab/Simulink

shaping in advance. All these controllers use feedforward information in order to decrease the position error. These three controllers will be discussed briefly below.

Learning controller

The first category discussed are learning controllers. This category can be subdivided into supervised learning, unsupervised learning, and reinforcement learning controllers. The advantage of this type of control is that not much knowledge about the system and the controller is needed. The controller can learn from a supervisor, which can be a motorcyclist, or it can learn by itself with the aid of reward and punishment, where the reward is given by the controller itself. A reward could be given every time the system meets a target, for example the completion of a corner, or a lap. A punishment could be given every time the system falls, or runs off the track. A problem of this type of control is that a large storage capacity is needed. Every action and reward combination for every state need to be stored. since there are 22 components and each state can obtain infinitely many values, this way of controlling will need a lot of storage capacity.

Model predictive controller

A second class of controllers are the model predictive controllers. A model predictive controller has the initial state of the system, and from that state, it tries several control inputs, and calculates what the predicted outcome of the model is. This controller also includes an optimization criterion that is not easy to formulate. Since an accurate model of the motorcycle exists, this way of controlling seems feasible. The controller should run the model far enough to be able to reach any desired state within the control horizon. In practice, this means that the controller should for example calculate five seconds in advance. Several control inputs have to be tried, so the model has to be simulated several times before the next state is available, which will be on a regular basis. The problem now becomes processing power. To run the model several times with a virtual timespan of 5 seconds, and do this within a fraction of a seconds demands a lot of processing power.

Reference signal tracking controller

The third type of control is the reference signal tracking controller. Data about the track, together with some information about the motorcycle is converted to a set of reference state signals. These reference signals describe what the most important states of the motorcycle should be as a function of time. During a lap, the actual state is then compared with the reference state, and a proportional action is taken based on the error. The advantage of this controller is that any error can be minimized, albeit only if the reference trajectory can be realized. Camber angle can be fed back towards the steering torque, but also the lateral position of the motorcycle on the track can be fed back towards the steering torque. One disadvantage is that all signals are a function of time. Starting a corner for example, is time based, and not position based. This means that if the longitudinal position on the track is not at the right place at the right time, the motorcycle will start cornering when not desired. This problem is solved by feeding back the longitudinal position to the engine torque with a proportional gain, so that the longitudinal position of the motorcycle is accurately defined with respect to time.

With a virtual track, the camber tracking controller can be optimized manually. Therefore, next section introduces a virtual track.

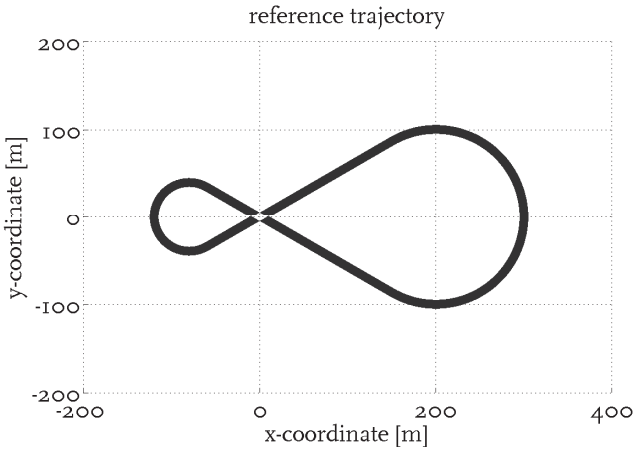

Figure 5.2: top view of the virtual track

5.2 Introduction of the virtual track

Figure 5.2 shows a top view of the virtual track. The track is 8 meters wide, and has two corners. The track has been chosen in such a way, that with a constant forward velocity of 20 meter per second, one corner will be taken at a camber angle of approximately 30 degrees, and the other corner wil be taken at a camber angle of around 60 degrees. A controller for this track has been designed. First, the track is analyzed to see what the different states of the motorcycle should be as a function of time. This track has been used since it is simple, but contains some important transitions from straight running to cornering, and back.

5.3 Analysis of the virtual track

The motorcycle model basically needs two input signals in order to be fully controlled. One signal determines the steering torque in time, and the other determines the wheel torque. The latter signal is then converted to a signal for the engine and the brakes. To keep the analysis simple, the forward velocity is controlled to be 20 meter per second. With this assumption, the most important states of the motorcycle model can be calculated as a function of time. Important states are position, velocity, yaw, yaw rate, camber and camber velocity.

Transition times

The track basically consists of two straight lines, and two arcs. The moment that the motorcycle is at the beginning of a straight line or an arc is called a transition moment. There are four transition moments, and with a constant forward velocity of 20 meters per second, these time instances can easily be calculated. The length of the first straight is calculated to be $100\sqrt{3}$ meter, and with 20 meters per second, it will take $5\sqrt{3}$ seconds to cross that distance. The first transition moment is therefore at $t_1 = 5\sqrt{3}$. The next piece of track is an arc, that is two third of a circle with a radius of 100 meter, and has a length of $\frac{400}{3}\pi$ meter. With a velocity of 20 meter per second, it takes $\frac{20}{3}\pi$ seconds to cross that distance, and $t_2 = 5\left(\sqrt{3} + \frac{4}{3}\pi\right)$ is thus the second transition moment. Then, a long straight has to be crossed. The length of that straight is $140\sqrt{3}$ meter, and will be traveled in $7\sqrt{3}$

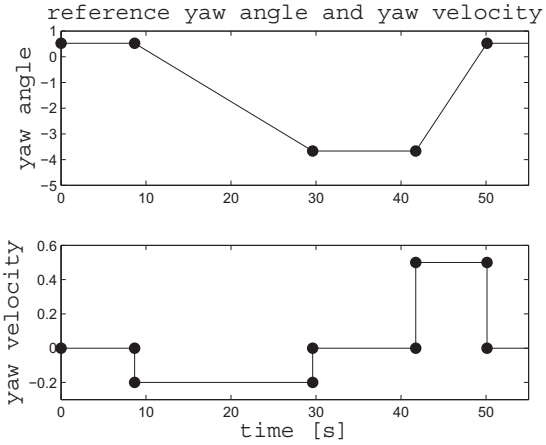

Figure 5.3: coarse reference yaw angle and yaw velocity

second. Therefore, the third transition moment is at $t_3 = 12\sqrt{3} + \frac{20}{3}\pi$. Then a sharp left corner is entered. this corner is $\frac{160}{3}\pi$ meter, or $\frac{8}{3}\pi$ second. The forth transition moment is at $t_4 = \frac{28}{3}\pi + 12\sqrt{3}$ With the final straight, the total track should be covered in $t_5 = \frac{28}{3}\pi + 14\sqrt{3}$ seconds. The transition moments are also summarized in table 5.1

Table 5.1: definition of the virtual track

section	duration	Transition moment	Transition time
straight	8.66	t_1	8.66
corner	20.94	t_2	29.60
straight	12.12	t_3	41.73
corner	8.38	t_4	50.11
straight	3.46	t_5	53.57

States as function of time

The important states should be available as a function of time in order to compare the real state with the referenced state. The first state to be analyzed for this track is the yaw angle. On a straight section, the yaw has a constant value. On the first straight, this constant yaw angle is 30 degrees, or $\frac{1}{6}\pi$ radians. In the next section, the yaw changes linearly from $\frac{1}{6}\pi$ radians, to $-\frac{7}{6}\pi$. Then, during the long straight, the yaw will stay $-\frac{7}{6}\pi$ radians. In the final corner, the yaw wil go back linearly from $-\frac{7}{6}\pi$ to $\frac{1}{6}\pi$ radians. With the yaw as function of time given, the yaw rate can be calculated as the derivative of the yaw. The yaw angle and yaw velocity are plotted in Figure 5.3.

In Figure 5.3, the dots mark moments that were calculated in the previous paragraph. At these moments marked by a dot, the derivative is undefined since the slope of the signal changes instantaeuos. It is assumed that the camber angle of the motorcycle is directly linked to the yaw velocity. A step in the yaw velocity therefore also means a step in the camber angle, which is undesirable, since it is not possible in reality. Therefore, the yaw velocity will be smoothed before calculating the other reference states.

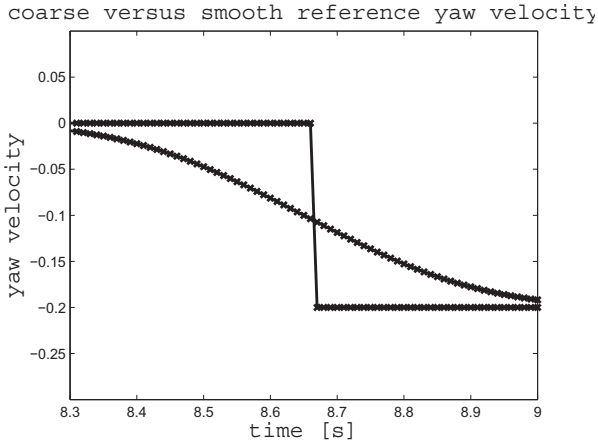

Figure 5.4: coarse reference yaw rate versus smooth yaw rate

Smoothing of the reference signal

Smoothing the yaw velocity reference signal is done in two steps. First, the time increments are reduced to steps of ten milliseconds. Next, the original yaw velocity is replaced with the average of all points 0.2 seconds before and after that particular point (moving average). The averaging is done with a gaussian weighing factor, to make points close to the particular point more important. The result of this first step in the yaw velocity can be seen in Figure 5.4. Note that smoothing the yaw velocity changes the path in the ground plane. It can be observed that this change is well within the track boundaries, and therefore does not cause problems in this case. For other tracks, the smoothed path should always be compared with the real path to see wether the smoothing has changed the path outside the track edges or not.

$$\begin{aligned} \dot{x}_0^{ref} &= 20\cos(q_0^{ref}) \\ \dot{y}_0^{ref} &= 20\sin(q_0^{ref}) \end{aligned} \tag{5.1}$$

From the smoothed yaw velocity, all other signals are derived. The smooth yaw reference angle is simply the integral of the smoothed yaw velocity. The reference velocity in x- and y- direction are calculated with (5.1). In (5.1), the number (20) stems from the forward velocity of the motorcycle, that always should be 20 meter per second. The position in x- and y- direction is again the integral of the velocity in x- respectively y- direction. The reference position and velocity in x- and y- direction are converted to a reference position and velocity in lateral and longitudinal direction with (5.2).

$$\begin{aligned} x_t^{ref} &= -\sin(q_0^{ref})x_0^{ref} + \cos(q_0^{ref})y_0^{ref} \\ x_l^{ref} &= \cos(q_0^{ref})x_0^{ref} + \sin(q_0^{ref})y_0^{ref} \\ v_t^{ref} &= -\sin(q_0^{ref})\dot{x}_0^{ref} + \cos(q_0^{ref})\dot{y}_0^{ref} \\ v_l^{ref} &= \cos(q_0^{ref})\dot{x}_0^{ref} + \sin(q_0^{ref})\dot{y}_0^{ref} \end{aligned} \tag{5.2}$$

Calculating the other reference states

The most important state for the motorcycle to stay controllable, is the camber angle. This state is a good indication wether the motorcycle is stable or not. The camber angle as function of time cannot

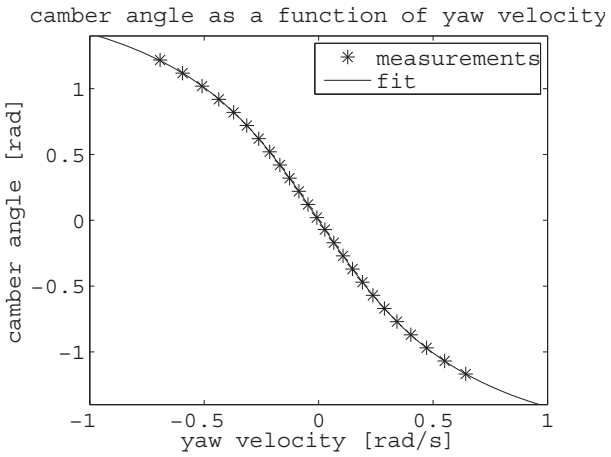

Figure 5.5: camber angle as a function of yaw velocity

be calculated with the track data alone. From simple inverted pendulum equilibrium, the camber angle can be estimated. The camber angle could also be called from a lookup table. The steady state camber angle has been plotted against the steady state yaw velocity in Figure 5.5. The camber angle as a function of yaw velocity is best described with the arctan function in (5.3). This equation has been obtained by nonlinear curve fitting. The curve fit can also be seen in Figure 5.5. The camber velocity reference signal is also calculated. That is done by differentiating the camber angle with respect to time.

$$q_1^{ref} = -1.279 \arctan(\dot{q}_0^{ref} 2.01) \tag{5.3}$$

Four reference trajectories are derived, together with their derivatives. In total, this counts up to eight signals. These signals are the lateral position, the longitudinal position, the camber angle, the yaw angle, and the derivatives of all these signals. From these signals, camber angle is the most important for the motorcycle to be stable. All signals are derived from the smoothed yaw velocity signal. The next section discusses how these signals will be fed to the system.

5.4 The controller

The controller is a simple proportional gain feedback controller. The reference state is compared with the real state, and a proportional control action is taken. The longitudinal position and velocity are fed back to the motorcycle engine torque, the other signals are fed back to the steering torque. It is interesting to see that two seemingly completely different things can be connected by a simple feed back loop. The controller is stated in (5.4). Note that the motorcycle longitudinal velocity reference signal is constant equal to 20 meter per second, and can thus be replaced by this number.

$$\begin{aligned} u_1 = \; & G_{q_0}\left(q_0^{ref} - q_0\right) + G_{\dot{q}_0}\left(\dot{q}_0^{ref} - \dot{q}_0\right) + G_{q_1}\left(q_1^{ref} - q_1\right) + \\ & G_{\dot{q}_1}\left(\dot{q}_1^{ref} - \dot{q}_1\right) + G_{x_t}\left(x_t^{ref} - x_t\right) + G_{v_t}\left(v_t^{ref} - v_t\right) \\ u_2 = \; & G_{x_l}\left(x_l^{ref} - x_l\right) + G_{v_l}\left(v_l^{ref} - v_l\right) \end{aligned} \tag{5.4}$$

The controller uses eight proportional gains. The gains are obtained by trial and error. These gains are thus not optimized. It is important to know that some gains can have an upper limit before the system becomes unstable, others can have a lower limit before the system becomes unstable. There is no rigorous proof that the system will be stable at all times, that is, an arbitrary initial condition, with these gains.

Table 5.2: Gains used in the controller to stabilize the motorcycle

name	value
G_{q_0}	1000
$G_{\dot{q}_0}$	100
G_{q_1}	-1000
$G_{\dot{q}_1}$	-100
G_{x_t}	200
G_{v_t}	200
G_{x_l}	1000
G_{v_l}	1000

A simulation done with the gains summarized in table 5.2 is described in the next section. One could ask wether these gains are realistic, and wether these gains are not too high to be implemented on a real motorcycle without the motor becoming unstable. This question can only be answered by experiments. Still, it is meaningful to investigate the system with this controller, even if the gains may be unrealistically high. A torque signal is obtained by simulating the motorcycle with this controller. That torque signal can be used as a feed forward signal to the real motorcycle without the problems of measurement noise. Therefore, the simulation of the controller in the next section is useful.

5.5 Evaluation of the controller

A simulation of the model with the controller and the track data is made. The resulting output states are visualized in a movie that shows the motorcycle and the track in virtual reality. In this virtual environment, the reference trajectory is visualized with a ghost. This ghost exactly follows the reference trajectory, and has no dynamics or physics engine. It behaves "unnatural". The visualization by means of a virtual model and a ghost is a very meaningful way of representing the different states as a function of time. The difference between the dynamic model and the reference trajectory can be seen in one glance. In this report, the different states that are important are plotted against time, together with the reference trajectories. The different important states are plotted for the full length of time in figure 5.6. The important control signals are the engine torque, and the steering torque. these signals, together with the steering velocity and steering angle are plotted in Figure 5.7.

Figures 5.6 and 5.7 reveal some very interesting information. First of all, the reference lateral velocity is zero over the whole track. The real lateral velocity is not zero while cornering. This is actually quite logic, since the lateral tire force is a function of the lateral tire velocity. Furthermore, to start a right turn, the motorcycle actually has to turn left first, and vice versa. The simulation shows that the motorcycle can follow the lateral and longitudinal position of the reference trajectory within centimeters accuracy. The torque applied to the steering head and the torque applied by the engine are plotted in Figure 5.7. These figures show that the applied torque has a realistic value.

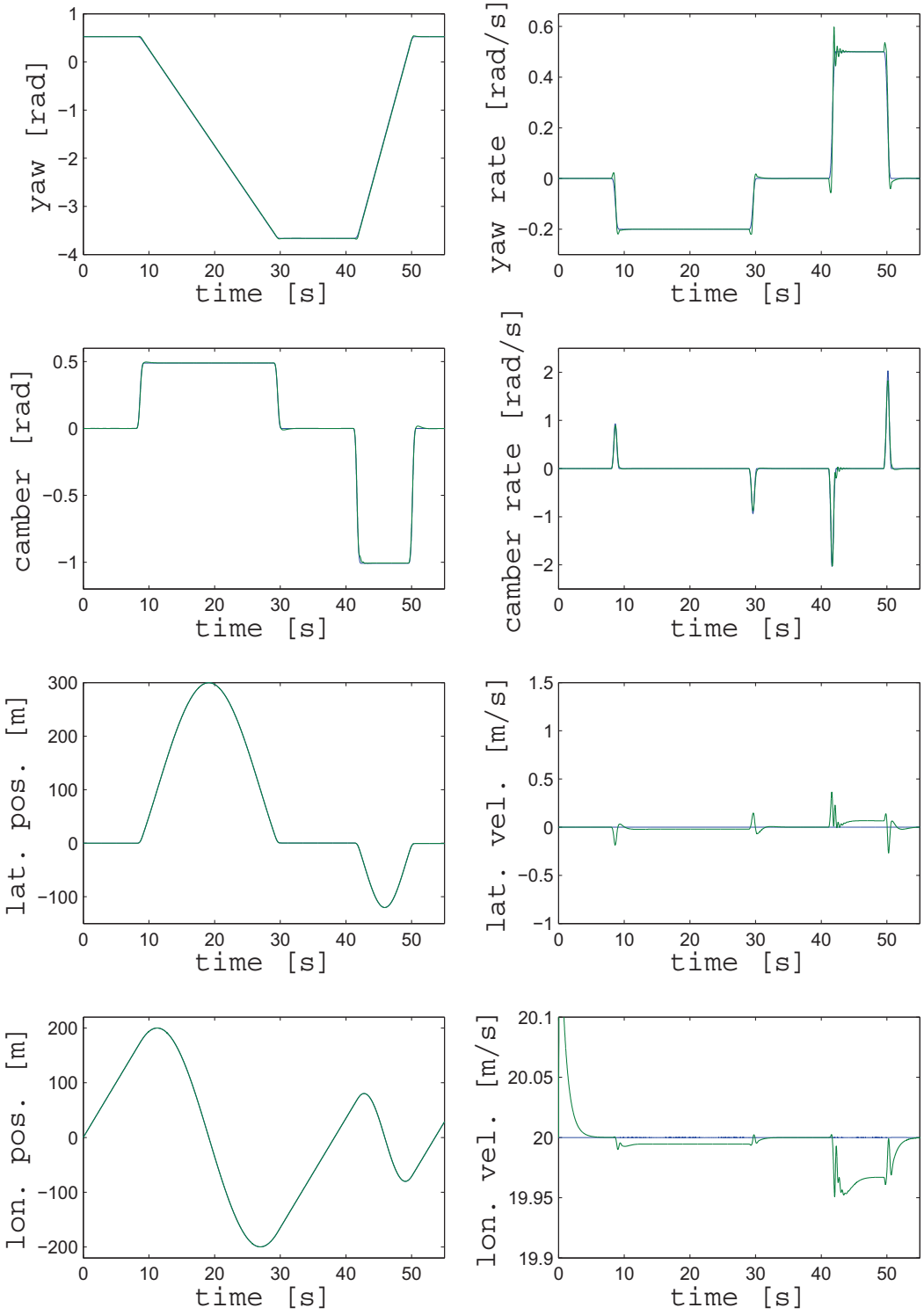

Figure 5.6: important components of the model as a function of time

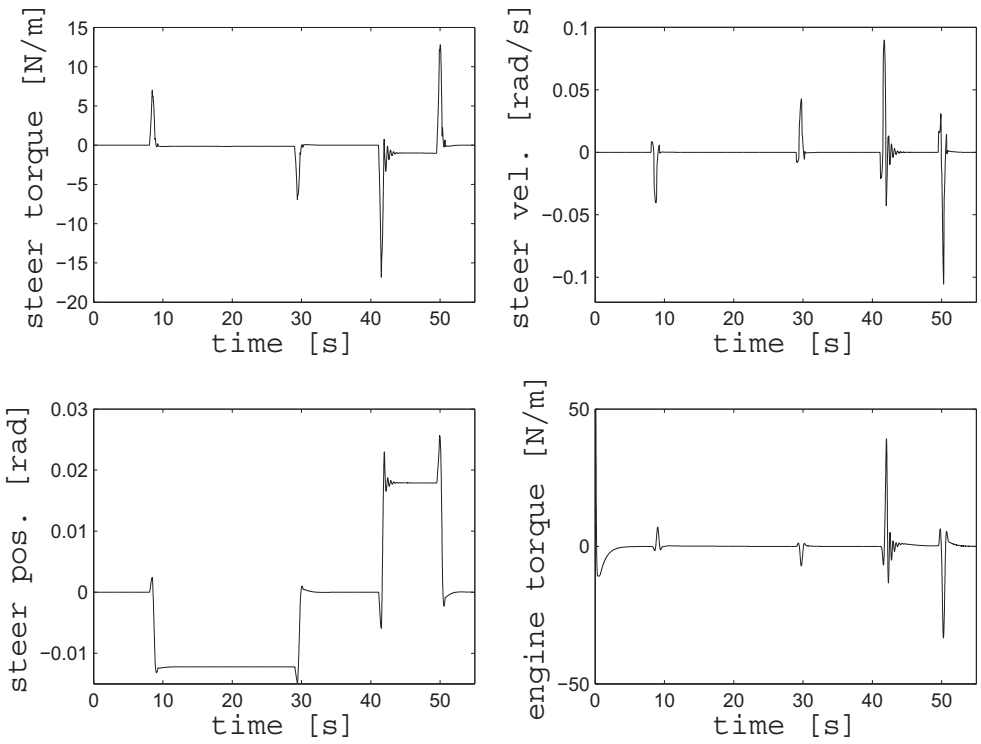

Figure 5.7: important components of the model as a function of time

5.6 A real track as a reference signal

For a real track, that is, a track that exists in real life somewhere on the globe, several major issues still have to be solved. first, the motorcycle should be able to have a variable forward velocity. As the forward velocity changes, so does the camber angle as a function of the yaw rate. second, the motorcycle starts from a standstill, which is an unstable situation independent of the control algorithm used. Finally, the states have to be measured. Measuring the states will automatically induce noise into the system. All these problems can be investigated and solved. In the final section, the yaw rate as a function of camber angle and forward speed is explained.

5.6.1 Camber as function of yaw rate and forward velocity

The function that describes the steady state camber angle is given as

$$q_1^{ss} = a_1 \arctan(a_2 \cdot \dot{q}_0^{ss} \cdot \sqrt{\dot{x}_0^{ss} + \dot{y}_0^{ss}}) \tag{5.5}$$

In (5.5), $\dot{q}_0^{ss}$ is the (steady state) yaw rate, and $\sqrt{\dot{x}_0^{ss} + \dot{y}_0^{ss}}$ is the total (steady state) velocity. a_1 And a_2 are constants that have small correction factors included. With the current set of parameters, these constants are best described as

$$a_1 = \frac{-0.62}{\sqrt{\dot{x}_0^{ss} + \dot{y}_0^{ss}} - 3.13} - 1.24 \qquad a_2 = \frac{-0.072}{\sqrt{\dot{x}_0^{ss} + \dot{y}_0^{ss}} - 2.36} + 0.1 \tag{5.6}$$

Equations (5.5) and (5.6) are accurate for camber angles between -70 and 70 degrees, and for all forward velocities between 4 m/s and 100 m/s. In a variable forward velocity reference trajectory, other boundary conditions should be set, in order to find the (time dependent) velocity signal. For straight line driving, the velocity is dependent of the maximum acceleration before the bike wil flip over backwards, and the maximum deceleration before the bike wil flip over forward. These values are obtained by simulating the model.

Chapter 6

Conclusion and recommendation

6.1 Conclusion

The problem statement of this graduation project is to make a motorcycle model that is accurate enough to predict motorcycle behavior at extreme driving conditions. An 11 degree of freedom motorcycle model has been developed, together with a controller that is able to follow a suitable reference trajectory within centimeters of accuracy. The way of model derivation is borrowed from robot modeling, and has been proved by this report to be a good way of motorcycle modeling. The model is comprehensive and small enough to be implemented and simulated real time, yet it is accurate enough to predict the complete configuration of the motorcycle as a function of time. Therefore, the research question of creating an accurate model is solved. The model shows that a motorcycle is controllable in theory. The model also shows that care must be taken when deriving the equations of motion, since it is easy to introduce errors in the model.

A proportional gain feedback controller is able to stabilize the motorcycle. The proportional gain feedback controller is also able to follow a reference trajectory in the ground plane. To do this, the reference trajectory is first transformed into a reference trajectory for the camber angle of the motorcycle rear wheel.

6.2 Recommendation

To use the full potential of this motorcycle model, the parameters of a real bike that is to be controlled should be measured scientifically. Measurement of the approximately 70 parameters should be done accurately, or else the complex model is useless. With rough estimated parameters, one could better use a much simpler motorcycle model. With accurate parameters, the boundaries on the motorcycle performance can be used to design the controller. Unlike the states, the parameters can be measured once and off line. The states should be measured on line and real time while controlling the motorcycle. The next step would be to investigate how accurate, and how often the states of the motorcycle should be measured, and what is the effect of noise in the signal on the controller performance. Not all states can be measured directly, but have to be calculated from other measurements. Therefore, the different measuring techniques should be examined and judged.

The obvious step to be taken after the previous research that is devoted to the feasibility of a rider-

less motorcycle, is to order the sensors and implement them on the motorcycle. The sensors should be connected to an onboard electronic control unit (ECU), that also embeds the motorcycle model. Preferably, the ECU is able to communicate with a laptop so that the different signals can be monitored. DSpace is probably too heavy and bulky to be used. Ethercad is a good alternative. If possible, the ECU is a dedicated system with all the electronics integrated. Maybe the ECU from Magneti Marelli used in Formula One cars can be used. Actuation of the steering axis, throttle, brake, gears and clutch should be automated. An algorithm that changes the requested engine torque to a throttle/clutch/shift signal should be elaborated. In short, the recommendations can be summarized as follows:

- measure parameters on a real bike
- research the effect of state measurement inaccuracy on controller performance
- select and implement sensors that measure the states, or develop a state estimator.
- automate the actuation of the steer, brake, throttle, gear, and clutch.
- implement the control unit
- embed the control software

Bibliography

[1] J. P. Meijaard A. L. Schwab and J. M. Papadopoulos. Benchmark results on the linearized equations of motion of an uncontrolled bicycle. *Proc. Second Asian Conference on Multibody Dynamics.*, pages 1–9, August 2004.

[2] D.H. van Campen B. de Kraker. *Mechanical Vibrations.* Shaker Publishing, 2001.

[3] E. Carvallo. Theorie du mouvement du monocycle et de la bicyclette. *Paris: Gauthier-Villars*, 1899.

[4] V. Cossalter. *Motorcycle Dynamics.* Greendale, second edition edition, 2006.

[5] C. de Wit. Dynamic tire friction models for vehicle traction control. *38th IEE-CDC*, 1999.

[6] E. Döhring. *Über die Stabilität und Lenkkräfte von Einspuhrfahrzeugen*. PhD thesis, University of Technology, Braunschweig, 1954.

[7] Klein F and Sommerfeld A. Uber die theorie des kreisels. *Stabilitat des Fahrrads*, page 863–884, 1910.

[8] W. Suhr F. Ries G. Franke. An advanced model of bicycle dynamics. *Eur. J. Phys*, 11:116–121, June 1989.

[9] N. H. Getz. Control for an autonomous bicycle. *IEEE International Conference on Robotics and Automation*, pages 1397–1402, 1995.

[10] Chih-Lyang Hwang. Fuzzy sliding-mode underactuated control for autonomous dynamic balance of an electrical bicycle. *IEEE transactions on control systems technology*, 17(3):658–670, 5 2009.

[11] P. Kessler. Motorcycle navigation with two sensors. Master's thesis, Department of Mechanical Engineering, University of California at Berkeley, 2004.

[12] C. Koenen. The dynamic behaviour of a motorcycle when running straight ahead and when cornering. *Doctoral Dissertation*, 1983. Delft University.

[13] Sharp R.S. Limebeer, D.J.N. Bicycles, motorcycles and models. *IEEE Contr. Syst. Mag.*, 26:34–61, 5.

[14] M.Vidyasagar M. W. Spong, Seth Hutchingson. *Robot Modeling and Control.* New York: Wiley, 2005.

[15] J.P. Meijaard, J.M. Papadopoulos, A. Ruina, and A.L. Schwab. Linearized dynamics equations for the balance and steer of a bicycle: a benchmark and review. *The Royal Society*, (463):1955–1982, June 2007.

[16] H. B. Pacejka. *Tyre and Vehicle Dynamics.* Elsevier Ltd., second edition edition, 2006.

[17] S. Evangelou R.S. Sharp and D.J.N. Limebeer. Advances in the modelling of motorcycle dynamics. *Electrical and Electronic Engineering*, 2004.

[18] P. A. Seiniger. *Erkennbarkeit und Vermeidbarkeit von ungebremsten Motorrad-Kurvenunfällen*. PhD thesis, Technischen Universität Darmstadt, 2009.

[19] Sharp. Stability, control and steering responses of motorcycles. *Vehicle System Dynamics*, 35(4-5):291–318, 2001.

[20] R.S. Sharp. The stability and control of motorcycles. *J. mech. Engn. Sci.*, 13(5):117–120, 1971.

[21] Y. Tanaka and T. Murakami. Self sustaining bicycle robot with steering controller. *Proceedings of 2004 IEEE Advanced Motion Control Conference*, pages 193–197, 2004.

[22] R. Lot V. Cossalter. A motorcycle multi-body model for real time simulations based on the natural coordinates approach. *Vehicle System Dynamics*, 37(6):423–447, 2002.

[23] N. van de Wouw. *Multibody Dynamics*. Lecture Notes, 2005.

[24] R. van Dooren. Motion of a rolling disk by a new generalized hamilton-jacobi method. *Journal of Applied Mathematics and Physics*, 27:501–505, 1976.

[25] N. P. Mansour W. B. Ribbens. *Understanding automotive electronics*. Elsevier Science, sixth edition edition, 2003.

[26] W.D.Versteden. Improving a tyre model for motorcycle simulations. final report, Eindhoven University of Technology, 2005.

[27] F. J. W. Whipple. The stability of the motion of a bicycle. *Quarterly Journal of Pure and Applied Mathematics*, 30:312–348, 1899.

[28] Levandowski Yi, Song. Trajectory tracking and balance stabilization control of autonomous motorcycles. *IEEE international conference on robotics and automation*, 5 2006.

Appendix A

Joint position vectors

The joint position vectors are stated in Eq. (??), and can be calculated explicitly to be:

Rear wheel contact patch

$$O_0 = \begin{bmatrix} x_0 \\ y_0 \\ z_0 \end{bmatrix}$$

Lowest point of the rear wheel torus centerline

$$O_1 = \begin{bmatrix} x_0 \\ y_0 \\ z_0 + c_r \end{bmatrix}$$

Rear wheel hub

$$O_2 = \begin{bmatrix} x_0 + s_0 s_1 b_r \\ y_0 - c_0 s_1 b_r \\ z_0 + c_r + c_1 b_r \end{bmatrix}$$

Swingarm joint position

$$O_3 = \begin{bmatrix} x_0 + c_0 c_6 d_4 + s_0 s_1 (b_r - s_6 d_4) \\ y_0 + s_0 c_6 d_4 - c_0 s_1 (b_r - s_6 d_4) \\ z_0 + c_r + c_1 (b_r - s_6 d_4) \end{bmatrix}$$

Steering joint position

$$O_4 = \begin{bmatrix} x_0 + c_0(c_6 d_4 + c_2 d_1) + s_0 s_1(b_r - s_6 d_4 - s_2 d_1) \\ y_0 + s_0(c_6 d_4 + c_2 d_1) - c_0 s_1(b_r - s_6 d_4 - s_2 d_1) \\ z_0 + c_r + c_1(b_r - s_6 d_4 - s_2 d_1) \end{bmatrix}$$

Front wheel hub position

$$O_5 = \begin{bmatrix} x_0 + c_0 * (c_6 d_4 + c_2(d_1 + c_3 d_3) - s_2 d_2) - s_0(c_1 s_3 d_3 - s_1(b_r - s_6 d_4 - s_2(d_1 + c_3 d_3) - c_2 d_2)) \\ y_0 + s_0(c_6 d_4 + c_2(d_1 + c_3 d_3) - s_2 d_2) + c_0(c_1 s_3 d_3 - s_1(b_r - s_6 d_4 - s_2(d_1 + c_3 d_3) - c_2 d_2)) \\ z_0 + c_r + s_1 s_3 d_3 + c_1(b_r - s_6 d_4 - s_2(d_1 + c_3 d_3) - c_2 d_2) \end{bmatrix}$$

Appendix B

Object position vectors

m_1; **rear wheel mass**

The vector pointing to the rear wheel mass center is similar as the vector pointing to the rear wheel hub. $Om_1 = O_2 = O_1 + R_0R_1 \begin{bmatrix} 0 \\ 0 \\ d_r - c_r \end{bmatrix} = \begin{bmatrix} x_0 + s_0 s_1 b_r \\ y_0 - c_0 s_1 b_r \\ z_0 + c_r + c_1 b_r \end{bmatrix}$

Orientation of the rear wheel

The orientation of the rear wheel is a combination of consecutively yaw, camber and rear wheel rotation.

$$Rm_1 = R_0R_1R_9 = \begin{bmatrix} c_0\ c_9 - s_0\ s_1\ s_9 & -s_0\ c_1 & c_0\ s_9 + s_0\ s_1\ c_9 \\ s_0\ c_9 + c_0\ s_1\ s_9 & c_0\ c_1 & s_0\ s_9 - c_0\ s_1\ c_9 \\ -c_1\ s_9 & s_1 & c_1\ c_9 \end{bmatrix}$$

Orientation of the swingarm

$$Rm_2 = R_0R_1R_6 = \begin{bmatrix} c_0\ c_6 - s_0\ s_1\ s_6 & -s_0\ c_1 & c_0\ s_6 + s_0\ s_1\ c_6 \\ s_0\ c_6 + c_0\ s_1\ s_6 & c_0\ c_1 & s_0\ s_6 - c_0\ s_1\ c_6 \\ -c_1\ s_6 & s_1 & c_1\ c_6 \end{bmatrix}$$

Orientation of the main body

The orientation of the main body is a combination of consecutively yaw, camber and pitch.

$$Rm_3 = R_0R_1R_2 = \begin{bmatrix} c_0\ c_2 - s_0\ s_1\ s_2 & -s_0\ c_1 & c_0\ s_2 + s_0\ s_1\ c_2 \\ s_0\ c_2 + c_0\ s_1\ s_2 & c_0\ c_1 & s_0\ s_2 - c_0\ s_1\ c_2 \\ -c_1\ s_2 & s_1 & c_1\ c_2 \end{bmatrix}$$

Orientation of the steering head

$$Rm_4 = R_0 R_1 R_2 R_3 = \begin{bmatrix} (c_0\ c_2 - s_0\ s_1\ s_2)\ c_3 - s_0\ c_1\ s_3 & -(c_0\ c_2 - s_0\ s_1\ s_2)\ s_3 - s_0\ c_1\ c_3 & c_0\ s_2 + s_0\ s_1\ c_2 \\ (s_0\ c_2 + c_0\ s_1\ s_2)\ c_3 + c_0\ c_1\ s_3 & -(s_0\ c_2 + c_0\ s_1\ s_2)\ s_3 + c_0\ c_1\ c_3 & s_0\ s_2 - c_0\ s_1\ c_2 \\ -c_1\ s_2\ c_3 + s_1\ s_3 & c_1\ s_2\ s_3 + s_1\ c_3 & c_1\ c_2 \end{bmatrix}$$

Orientation of the front fork

$Rm_5 = Rm_4$

Orientation of the front wheel

$$Rm_6 = R_0 R_1 R_2 R_3 R_{10} =$$

$$\begin{bmatrix} \begin{array}{c}((c_0\ c2 - s_0\ s_1\ s_2)\ c_3 - s_0\ c_1\ s_3) \\ cX - (c_0\ s_2 + s_0\ s1\ c2)\ sX \\ + (c_0\ s_2 + s_0\ s1\ c2)\ cX\end{array} & -(c_0\ c2 - s_0\ s1\ s_2)\ s_3 - s_0\ c_1\ c_3 & ((c_0\ c2 - s_0\ s1\ s_2)\ c_3 - s_0\ c_1\ s_3)\ sX \\ \begin{array}{c}((s_0\ c2 + c_0\ s1\ s_2)\ c_3 + c_0\ c_1\ s_3)\ cX \\ - (s_0\ s_2 - c_0\ s1\ c2)\ sX \\ + (s_0\ s_2 - c_0\ s1\ c2)\ cX\end{array} & -(s_0\ c2 + c_0\ s1\ s_2)\ s_3 + c_0\ c_1\ c_3 & ((s_0\ c2 + c_0\ s1\ s_2)\ c_3 + c_0\ c_1\ s_3)\ sX \\ (-c_1\ s_2\ c_3 + s1\ s_3)\ cX - c_1\ c2\ sX & c_1\ s_2\ s_3 + s1\ c_3 & (-c_1\ s_2\ c_3 + s1\ s_3)\ sX + c_1\ c2\ cX \end{bmatrix}$$

Appendix C

Mass matrix

This appendix states the mass matrix. If an entry is not in the list, it must be zero. Note that the mass matrix is symmetric, and so $M_{ij} = M_{ji}$

$$
\begin{aligned}
M_{11} = \;& m_1 + m_2 + m_3 + m_4 + m_5 + m_6 \\
M_{14} = \;& m_1 c_0 s_1 b_r + m_2(-s_0(c_6 p_{2x} + s_6 p_{2z}) + c_0 s_1 a_{22}) + m_3(-s_0 a_{12} + c_0 s_1 a_{13}) + m_5(-s_0 a_5 - c_0 a_8) \\
& + m_4((-s_2 p_{4z} - c_6 d_4 - (d_1 + c_3 p_{4x}) c_2) s_0 - c_0(c_1 s_3 p_{4x} - s_1 a_{11})) + m_6(-s_0 a_2 - c_0(c_1 s_3 d_3 - s_1 a_3)) \\
M_{15} = \;& m_1 s_0 c_1 b_r - m_4 s_0(-s_1 s_3 p_{4x} - c_1 a_{11}) - m_6 s_0(-s_1 s_3 d_3 - c_1(d_r - c_r - s_6 d_4 - s_2(d_1 + c_3 d_3) - c_2 d_2) - c_r) \\
& + m_3 s_0 c_1 a_{13} + m_2 s_0 c_1 a_{22} - m_5 s_0(-s_1 s_3(d_3 + p_{5x}) - c_1(d_r - c_r - s_6 d_4 - a_6 + c_2(-d_2 + p_{5z})) - c_r) \\
M_{16} = \;& m_3(c_0(-s_2 p_{3x} + c_2 p3z) + s_0 s_1(-c_2 p_{3x} - s_2 p3z)) + m_4(c_0 a_{21} + s_0 s_1 a_{19}) \\
& + m_5(c_0(-a_6 + c_2(-d_2 + p_{5z})) + s_0 s_1(-a_4 - s_2(-d_2 + p_{5z}))) + m_6(c_0 a_{20} + s_0 s_1 a_9) \\
M_{17} = \;& m_4(-s_3 p_{4x} c_2 c_0 - s_0 a_{18}) + m_5(-c_0 c_2 s_3(d_3 + p_{5x}) - s_0 a_{17}) + m_6(-c_0 c_2 s_3 d_3 - s_0 a_{18}) \\
M_{18} = \;& m_2(c_0(-s_6 p_{2x} + c_6 p_{2z}) + s_0 s_1(-c_6 p_{2x} - s_6 p_{2z})) + m_3 a_{15} + m_4 a_{15} + m_5 a_{15} + m_6 a_{15} \\
M_{19} = \;& m_5(-c_0 s_2 - s_0 s_1 c_2) + m_6(-c_0 s_2 - s_0 s_1 c_2) \\
M_{22} = \;& m_1 + m_2 + m_3 + m_4 + m_5 + m_6 \\
M_{24} = \;& m_1 s_0 s_1 b_r + m_2(c_0(c_6 p_{2x} + s_6 p_{2z}) + s_0 s_1 a_{22}) + m_3(c_0 a_{12} + s_0 s_1 a_{13}) \\
& + m_4(c_0 a_{10} - s_0(c_1 s_3 p_{4x} - s_1 a_{11})) + m_5(c_0 a_5 - s_0 a_8) + m_6(c_0 a_2 - s_0(c_1 s_3 d_3 - s_1 a_3)) \\
M_{25} = \;& -m_1 c_0 c_1 b_r - m_2 c_0 c_1 a_{22} - m_3 c_0 c_1 a_{13} + m_4 c_0(-s_1 s_3 p_{4x} - c_1 a_{11}) + m_5 c_0 a_{23} + m_6 c_0(-s_1 s_3 d_3 - c_1 a_3) \\
M_{26} = \;& m_3(s_0(-s_2 p_{3x} + c_2 p_{3z}) - c_0 s_1(-c_2 p_{3x} - s_2 p_{3z})) + m_4(s_0 a_{21} - c_0 s_1 a_{19}) \\
& + m_5(s_0(-a_6 + c_2(-d_2 + p_{5z})) - c_0 s_1(-a_4 - s_2(-d_2 + p_{5z}))) + m_6(s_0 a_{20} - c_0 s_1 a_9) \\
M_{27} = \;& m_4(-s_3 p_{4x} c_2 s_0 + c_0 a_{18}) + m_5(-s_0 c_2 s_3(d_3 + p_{5x}) + c_0 a_{17}) + m_6(-s_0 c_2 s_3 d_3 + c_0 a_{16}) \\
M_{28} = \;& m_2(s_0(-s_6 p_{2x} + c_6 p_{2z}) - c_0 s_1(-c_6 p_{2x} - s_6 p_{2z})) + m_3 a_{14} + m_4 a_{14} + m_5 a_{14} + m_6 a_{14} \\
M_{29} = \;& m_5(-s_0 s_2 + c_0 s_1 c_2) + m_6(-s_0 s_2 + c_0 s_1 c_2) \\
M_{33} = \;& m_1 + m_2 + m_3 + m_4 + m_5 + m_6 \\
M_{35} = \;& -m_1 s_1 b_r - m_2 s_1 a_{22} - m_3 s_1 a_{13} + m_4(c_1 s_3 p_{4x} - s_1 a_{11}) + m_5 a_8 + m_6(c_1 s_3 d_3 - s_1 a_3) \\
M_{36} = \;& m_3 c_1(-c_2 p_{3x} - s_2 p_{3z}) + m_4 c_1 a_{19} + m_5 c_1(-a_4 - s_2(-d_2 + p_{5z})) + m_6 c_1 a_9 \\
M_{37} = \;& m_4(s_1 c_3 p_{4x} + s_3 p_{4x} s_2 c_1) + m_5(s_1 c_3(d_3 + p_{5x}) + c_1 s_2 s_3(d_3 + p_{5x})) + m_6(s_1 c_3 d_3 + c_1 s_2 s_3 d_3) \\
M_{38} = \;& m_2 c_1(-c_6 p_{2x} - s_6 p_{2z}) - m_3 c_1 c_6 d_4 - m_4 c_1 c_6 d_4 - m_5 c_1 c_6 d_4 - m_6 c_1 c_6 d_4 \\
M_{39} = \;& -m_5 c_1 c_2 - m_6 c_1 c_2 \\
M_{44} = \;& m_1 s_1^2 b_r^2 + c_1^2(I_{1x} - I_{1y}) + I_{1y} + m_2((c_6 p_{2x} + s_6 p_{2z})^2 + s_1^2 a) 22^2) + c_1^2(c_6^2(I_{2z} - I_{2x}) + I_{2x} - I_{2y}) \\
& + I_{2y} + m_3(a_{12}^2 + s_1^2 a_{13}^2) + c_1^2(c_2^2(I_{3z} - I_{3x}) + I_{3x} - I_{3y}) + I_{3y} + m_4(a_{10}^2 + (c_1 s_3 p_{4x} - s_1 a_{11})^2) \\
& + c_1^2(c_2^2(I_{4z} - I_{4x}) + s_2^2 s_3^2(I_{4y} - I_{4x}) + c_3^2(I_{4x} - I_{4y})) + c_3^2(I_{4y} - I_{4x}) + 2 s_1 c_3 s_2 c_1 s_3(I_{4y} - I_{4x}) \\
& + I_{4x} + m_5(a_5^2 + a_5^2) + I_{5y} - (I_{5y} - I_{5x})(s_1 s_3 - c_1 c_3 s_2)^2 + c_1^2 c_2^2(I_{5z} - I_{5y}) \\
& + m_6(a_2^2 + (c_1 s_3 d_3 - s_1 a_3)^2) + I_{6x} + (I_{6y} - I_{6x})(s_1 c_3 + c_1 s_2 s_3)^2 \\
M_{45} = \;& m_2 c_1(-c_6 p_{2x} - s_6 p_{2z}) a_{22} + c_1 s_6 c_6(I_{2z} - I_{2x}) + m_3(-c_2 p_{3x} - s_2 p_{3z} - c_6 d_4) c_1 a_{13} \\
& + m_4 a_{10}(-s_1 s_3 p_{4x} - c_1 a_{11}) + c_2(c_1 s_2(I_{4z} - I_{4y} + c_3^2(I_{4y} - I_{4x})) + s_1 c_3 s_3(I_{4x} - I_{4y})) \\
& + m_5 a_5 a_{23} - c_2(s_1 c_3 s_3(I_{5y} - I_{5x}) + c_1 s_2(c_3^2(I_{5x} - I_{5y}) + I_{5y} - I_{5z})) \\
& + m_6 a_2(-s_1 s_3 d_3 - c_1 a_3) - c_2(-I_{6y} + I_{6x})(-s_1 c_3 s_3 - c_1 s_2 s_3^2) + c_1 s_2 c_2(I_{3z} - I_{3x}) \\
M_{46} = \;& m_3 s_1(-b_r s_2 p_{3x} + b_r c_2 p_{3z} + s_6 d_4 s_2 p_{3x} - s_6 d_4 c_2 p_{3z} + p_{3x}^2 + c_6 d_4 c_2 p_{3x} + c_6 d_4 s_2 p_{3z} + p_{3z}^2) \\
& + I_{3y} s_1 + m_4((-c_1 s_3 p_{4x} + s_1 a_{11}) a_{21} - a_{10} s_1 a_{19}) + s_1 I_{4x} + (I_{4y} - I_{4x}) c_3(s_1 c_3 + c_1 s_2 s_3) \\
& + s1_(I_{5x} + c_3^2(I_{5y} - I_{5x})) + c_1 c_3 s_3 s_2(I_{5y} - I_{5x}) \\
& + m_5((-c_1 s_3(d_3 + p_{5x}) + s_1 a_7)(-a_6 + c_2(-d_2 + p_{5z})) - a_5 s_1(-a_4 - s_2(-d_2 + p_{5z}))) \\
& + m_6((-c_1 s_3 d_3 + s_1 a_3) a_{20} - a_2 s_1 a_9) + s_1(c_3^2(I_{6y} - I_{6x}) + I_{6x}) + c_1 c_3 s_3 s_2(I_{6y} - I_{6x}) \\
M_{47} = \;& m_4((c_1 s_3 p_{4x} - s_1 a_{11}) c_2 s_3 p_{4x} + a_{10} a_{18}) + c_1 c_2 I_{4z} \\
& + m_5(a_8 c_2 s_3(d_3 + p_{5x}) + a_5 a_{17}) + c_1 c_2 I_{5z} + m_6((c_1 s_3 d_3 - s_1 a_3) c_2 s_3 d_3 + a_2 a_{16}) + c_1 c_2 I_{6x} \\
M_{48} = \;& m_2 s_1(b_r c_6 p_{2z} - b_r s_6 p_{2x} + p_{2z}^2 + p_{2x}^2) + I_{2y} s_1 + m_6((c_1 s_3 d_3 - s_1 a_3) s_6 d_4 + a_2 s_1 c_6 d_4) \\
& + m_4((c_1 s_3 p_{4x} - s_1 a_{11}) s_6 d_4 + a_{10} s_1 c_6 d_4) + m_5(a_8 s_6 d_4 + a_5 s_1 c_6 d_4) + m_3(-s_1 a_{13} s_6 d_4 + a_{12} s_1 c_6 d_4) \\
M_{49} = \;& m_5(a_8 s_2 + a_5 s_1 c_2) + m_6((c_1 s_3 d_3 - s_1 a_3) s_2 + a_2 s_1 c_2) \\
M_{410} = \;& s_1 I_{1y} \\
M_{411} = \;& I_{6y}(s_1 c_3 + c_1 s_2 s_3)
\end{aligned}
$$

$$
\begin{aligned}
M_{55} = \quad & m_1 b_r^2 + I_{1x} + m_2 a_{22}^2 + c_6^2(I_{2x} - I_{2z}) + I_{2z} + m_3 a_{13}^2 + c_2^2(I_{3x} - I_{3z}) + I_{3z} \\
& + m_4(s_3^2 p_{4x}^2 + a_{11}^2) + c_2^2(c_3^2(I_{4x} - I_{4y}) + I_{4y} - I_{4z}) + I_{4z} \\
& + m_5(s_3^2(d_3 + p_{5x})^2 + a_7^2) + I_{5z} + c_2^2(c_3^2(I_{5x} - I_{5y}) + I_{5y} - I_{5z}) \\
& + m_6(s_3^2 d_3^2 + a_3^2) + I_{6x} + c_2^2(c_3^2(-I_{6y} + I_{6x}) + I_{6y} - I_{6x}) \\
M_{56} = \quad & m_4 s_3 p_{4x} a_{19} + c_2 c_3 s_3(I_{4x} - I_{4y}) + m_5 s_3(d_3 + p_{5x})(-a_4 - s_2(-d_2 + p_{5z})) \\
& + c_2 c_3 s_3(I_{5x} - I_{5y}) + m_6 s_3 d_3 a_9 + c_2 c_3 s_3(-I_{6y} + I_{6x}) \\
M_{57} = \quad & m_4((-b_r + s_6 d_4 + (d_1 + c_3 p_{4x}) s_2 - c_2 p_{4z}) c_3 p_{4x} + s_3^2 p_{4x}^2 s_2) + I_{4z} s_2 \\
& + m_5((-b_r + s_6 d_4 + a_6 - c_2(-d_2 + p_{5z})) c_3(d_3 + p_{5x}) + s_3^2(d_3 + p_{5x})^2 s_2) \\
& + I_{5z} s_2 + m_6((-b_r + s_6 d_4 + s_2(d_1 + c_3 d_3) + c_2 d_2) c_3 d_3 + s_3^2 d_3^2 s_2) + s_2 I_{6x} \\
M_{58} = \quad & -m_4 s_3 p_{4x} c_6 d_4 - m_5 s_3(d_3 + p_{5x}) c_6 d_4 - m_6 s_3 d_3 c_6 d_4 \\
M_{59} = \quad & -m_5 s_3(d_3 + p_{5x}) c_2 - m_6 s_3 d_3 c_2 \\
M_{511} = \quad & -I_{6y} s_3 c_2 \\
M_{66} = \quad & m_3(p_{3z}^2 + p_{3x}^2) + I_{3y} + m_4(d_1^2 + 2 d_1 c_3 p_{4x} + c_3^2 p_{4x}^2 + p_{4z}^2) + c_3^2(I_{4y} - I_{4x}) + I_{4x} + c_3^2(I_{6y} - I_{6x}) \\
& + m_5((d_1 + c_3(d_3 + p_{5x}))^2 + (-d_2 + p_{5z})^2) + I_{5x} + c_3^2(I_{5y} - I_{5x}) + m_6((d_1 + c_3 d_3)^2 + d_2^2) + I_{6x} \\
M_{67} = \quad & -m_4 p_{4z} s_3 p_{4x} + m_5(d_2 - p_{5z}) s_3(d_3 + p_{5x}) + m_6 d_2 s_3 d_3 \\
M_{68} = \quad & m_3(d_4 p_{3x} cos(q_2 - q_6) + d_4 p_{3z} sin(q_2 - q_6)) + m_6((s_2(d_1 + c_3 d_3) + c_2 d_2) s_6 d_4 - a_9 c_6 d_4) \\
& + m_4(d_4 d_1 cos(q_2 - q_6) + \tfrac{1}{2} d_4 p_{4x} cos(q_2 - q_6 + q_3) + \tfrac{1}{2} d_4 p_{4x} cos(q_2 - q_6 - q_3) + d_4 p_{4z} sin(q_2 - q_6)) \\
& + m_5((a_6 - c_2(-d_2 + p_{5z})) s_6 d_4 - (-a_4 - s_2(-d_2 + p_{5z})) c_6 d_4) \\
M_{69} = \quad & m_5(d_1 + c_3(d_3 + p_{5x})) + m_6(d_1 + c_3 d_3) \\
M_{611} = \quad & I_{6y} c_3 \\
M_{77} = \quad & m_4 p_{4x}^2 + I_{4z} + m_5(d_3 + p_{5x})^2 + I_{5z} + m_6 d_3^2 + I_{6x} \\
M_{78} = \quad & m_4(s_3 p_{4x} c_2 s_6 d_4 - s_3 p_{4x} s_2 c_6 d_4) + m_6(s_3 d_3 c_2 s_6 d_4 - s_2 s_3 d_3 c_6 d_4) \\
& + m_5(s_3(d_3 + p_{5x}) c_2 s_6 d_4 - s_2 s_3(d_3 + p_{5x}) c_6 d_4) \\
M_{88} = \quad & m_2(p_{2x}^2 + p_{2z}^2) + I_{2y} + m_3 d_4^2 + m_4 d_4^2 + m_5 d_4^2 + m_6 d_4^2 \\
M_{89} = \quad & m_5 a_1 + m_6 a_1 \\
M_{99} = \quad & m_5 + m_6 \\
M_{1010} = \quad & I_{1y} \\
M_{1111} = \quad & I_{6y}
\end{aligned}
$$

In the mass matrix, there are 23 subexpressions:

$$
\begin{aligned}
a_1 = \quad & s_6 d_4 s_2 + c_6 d_4 c_2 \\
a_2 = \quad & c_6 d_4 + c_2(d_1 + c_3 d_3) - s_2 d_2 \\
a_3 = \quad & b_r - s_6 d_4 - s_2(d_1 + c_3 d_3) - c_2 d_2 \\
a_4 = \quad & c_2(d_1 + c_3(d_3 + p_{5x})) \\
a_5 = \quad & c_6 d_4 + c_2(d_1 + c_3(d_3 + p_{5x})) + s_2(-d_2 + p_{5z}) \\
a_6 = \quad & s_2(d_1 + c_3(d_3 + p_{5x})) \\
a_7 = \quad & b_r - s_6 d_4 - s_2(d_1 + c_3(d_3 + p_{5x})) + c_2(-d_2 + p_{5z}) \\
a_8 = \quad & c_1 s_3(d_3 + p_{5x}) - s_1(b_r - s_6 d_4 - s_2(d_1 + c_3(d_3 + p_{5x})) + c_2(-d_2 + p_{5z})) \\
a_9 = \quad & -c_2(d_1 + c_3 d_3) + s_2 d_2 \\
a_{10} = \quad & s_2 p_{4z} + c_6 d_4 + (d_1 + c_3 p_{4x}) c_2 \\
a_{11} = \quad & b_r - s_6 d_4 - (d_1 + c_3 p_{4x}) s_2 + c_2 p_{4z} \\
a_{12} = \quad & c_2 p_{3x} + s_2 p_{3z} + c_6 d_4 \\
a_{13} = \quad & b_r - s_6 d_4 - s_2 p_{3x} + c_2 p_{3z} \\
a_{14} = \quad & -s_0 s_6 d_4 + c_0 s_1 c_6 d_4 \\
a_{15} = \quad & -c_0 s_6 d_4 - s_0 s_1 c_6 d_4 \\
a_{16} = \quad & c_1 c_3 d_3 - s_1 s_2 s_3 d_3 \\
a_{17} = \quad & c_1 c_3(d_3 + p_{5x}) - s_1 s_2 s_3(d_3 + p_{5x}) \\
a_{18} = \quad & c_1 c_3 p_{4x} - s_1 s_3 p_{4x} s_2 \\
a_{19} = \quad & -(d_1 + c_3 p_{4x}) c_2 - s_2 p_{4z} \\
a_{20} = \quad & -s_2(d_1 + c_3 d_3) - c_2 d_2 \\
a_{21} = \quad & -(d_1 + c_3 p_{4x}) s_2 + c_2 p_{4z} \\
a_{22} = \quad & b_r - s_6 p_{2x} + c_6 p_{2z} \\
a_{23} = \quad & -s_1 s_3(d_3 + p_{5x}) - c_1(b_r - s_6 d_4 - s_2(d_1 + c_3(d_3 + p_{5x})) + c_2(-d_2 + p_{5z}))
\end{aligned}
$$

Appendix D

A different modelling approach

Another model has been made. This time, the model has thirteen degrees of freedom. The model will not be explained in detail in this report, but some remarks on this and the other model are discussed.

In the second model, q_3 is not a generalized coordinate anymore. Instead, q_8 has been taken as a generalized coordinate. Furthermore, q_4 and q_5 are also used as generalized coordinates, albeit with a slightly different meaning. Namely, q_4 and q_5 have opposite sign in the new model. With two extra generalized coordinates, two algebraic constraint equations should be included in the model. The mass orientation matrix and the two constraint equations are given in as

$$\begin{array}{rl} Rm_1 = & R_0 R_1 R_9 \\ Rm_2 = & R_0 R_1 R_6 \\ Rm_3 = & R_0 R_1 R_2 \\ Rm_4 = & R_8 R_5 R_4 \\ Rm_5 = & R_8 R_5 R_4 \\ Rm_6 = & R_8 R_5 R_{10} \end{array} \tag{D.1}$$

$$\begin{array}{l} 0 = \tan(q_1)\cos(q_0 - q_8) - \tan(q_2)\sin(q_0 - q_8)/\cos(q_1) - \tan(q_5) \\ 0 = \cos(q_1)\cos(q_2) - \cos(q_4)\cos(q_5) \end{array} \tag{D.2}$$

D.1 Comparison of both models

As can be seen in Equation D.1, the object orientations will have a minimum size of representation. The expressions for the forces from the front wheel contact patch will be much smaller. Although the mass and Christoffel matrix will increase from a square matrix of size eleven to a square matrix of size thirteen, The total character size of these matrices will decrease from 18.000 to 11.000 and from 100.000 to 80.000 respectively. In the previous model, the front wheel lateral and longitudinal force and moment took up 330.000 characters, while in this model, that figure is only 20.000. The total size of the equations of motion are much less than 200.000 characters.

The two extra constraint equations can be included in the model with Lagrange multipliers. If that is done, the ordinary differential equations (ode) transform in a set of differential algebraic equations (dae). Matlab cannot solve this set anymore because the index of this dae is more than one. To

circumvent that problem, the constraint equations can be put in the controller. with a high gain PD controller, the error can be kept small.

A high gain feedback means that the ode solver is forced to make small time steps. The time gained with the smaller equations of motion is then offset by the time lost in taking so many time steps. If a suitable dae were at hand, the second model would certainly be worth looking at.

Finally, the constraint equations could be left out, and replaced by a twisting and bending moment of the main frame. That solution is comparable with the feedback controller, and will probably need hight bending stiffness in order to be accurate.

Appendix E

Bicycle and Motorcycle Dynamics 2010 Poster

Technische Universiteit Eindhoven University of Technology

A motorcycle model for dynamic analysis

W. Ooms w.ooms@student.tue.nl
I.J.M. Besselink I.J.M.Besselink@tue.nl
H. Nijmeijer H.Nijmeijer@tue.nl

Department of Mechanical Engineering.

Introduction

A motorcycle model with 11 degrees of freedom has been derived. The model is a set of nonlinear differential equations that describe the motion of the motorcycle as a function of the forces acting on the separate bodies.

Unique features

The model derived differs from most models in the literature in that the rolling wheel is not modeled as a nonholonomic constraint, but includes a simple linear tire model, that is capable of predicting tire forces at large camber angles. Furthermore, the model is fully nonlinear and lateral and longitudinal dynamics are united. This is possible by using the same modeling method as is used in robot modeling [1]. The tire contact patches have a similar meaning as a robot's end effector.

The model

The model originates from Lagrange mechanics. The 11 degrees of freedom are:

- the head tube position and orientation (roll, pitch, yaw)
- the front and rear suspension
- the rotation angle of the wheels
- the steering angle

The six bodies included in the model are stated in the first column of Table 1. With these bodies included, there is a clear distinction between sprung and unsprung mass, and the unsprung mass is divided in a rotating and a fixed part.

Bodies included	Forces included
• the wheels	•steering torque
• the main frame	•engine torque
• the steering head	•brake torque
• the front fork	•suspension force
• the swingarm	•tire contact patch force

Table 1: summary of the bodies and forces included in the motorcycle model. The first three forces are used as control inputs.

Forces and torques included in the model are stated in the second column of table 1. With these forces included, the model can simulate wheelies, stoppies, weave, wobble, powerslides, highsiders, lowsiders, capsize, pitch, bounce, wheel hop and all other dynamic phenomena observed in real motorcycles.

Simulation and visualization

The model is implemented in Matlab/Simulink for simulation and visualization. Figure 1 shows a snapshot of the model visualization.

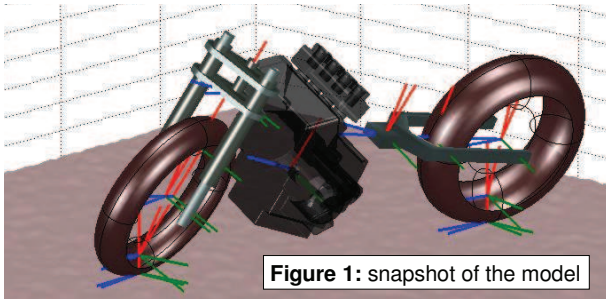

Figure 1: snapshot of the model

Linearization, analysis and validation

The model has been linearized and compared with the model of Koenen [2], and with the Jbike6 [3]. A bifurcation diagram is made where the eigenvalues are calculated for different forward speeds with the Koenen, and the Jbike6 parameters inserted in the model. Another set of parameters is used which represents a supersport motorcycle. Figure 3 shows a bifucation diagram with the unstable weave mode at low velocity, and capsize at high velocity. In between there is a stable regime. The model shows similar dynamics as the literature models from [2] and [3].

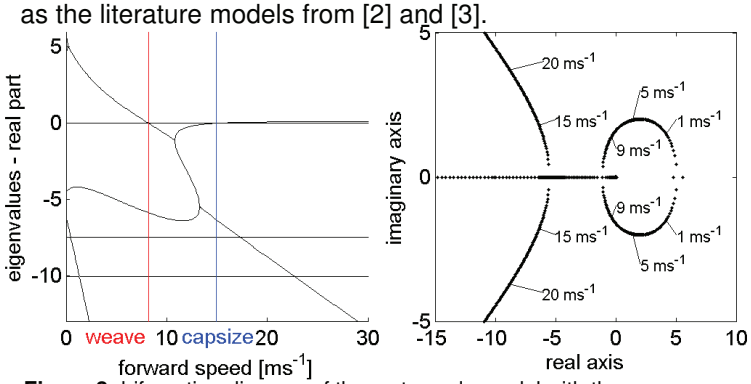

Figure 3: bifurcation diagram of the motorcycle model with the supersport motorcycle parameters inserted

Furthermore, the model is validated in the time domain with another nonlinear model made in SimMechanics. Both models show similar dynamics to machine precision accuracy.

References

[1] M. W. Spong, S. Hutchinson, and M. Vidyasagar, *Robot Modeling and Control*, John Wiley & Sons, Inc., New York, 2006.

[2] Koenen, C., *'The dynamic behaviour of a motorcycle when running straight ahead and when cornering'*, Doctoral Dissertation, Delft University, 1983.

[3] A. L. Schwab, J. P. Meijaard, and J. M. Papadopoulos, *"Benchmark results on the linearized equations of motion of an uncontrolled bicycle."* Proc. Second Asian Conference on Multibody Dynamics., pp. 1–9, August, 2004